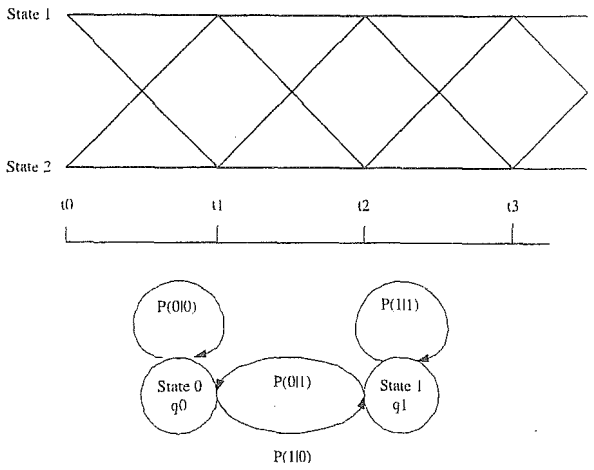

Fig. 4 Trellis diagram and state transition of HMM.

Table 2 Channel model and its parameters.

	CM1	CM2	CM3	CM4
p_{00}	$1-p_{01}$	$1-p_{01}$	$1-p_{01}$	$1-p_{01}$
p_{01}	0.06	0.5	0.06	0.06
p_{10}	0.017	0.5	0.017	0.017
p_{11}	$1-p_{10}$	$1-p_{10}$	$1-p_{10}$	$1-p_{10}$
$p_{00}(0)$	0.01	0.01	0.999	0.6
$p_{01}(0)$	0.5	0.5	0.9	0.4
$p_{10}(0)$	0.01	0.01	0.999	0.6
$p_{11}(0)$	0.5	0.5	0.9	0.4
BPSK	26.55%	25.5%	94.74%	49.57%
QPSK	73.45%	74.5%	5.26%	50.43%

both worst and better cases therefore we can show that proposed method can accommodate all the channel models by using these four typical channel models. In the EM based receiver, note that channel estimation error occurs which causes demodulator estimation error at Step 1 and 2 in Fig. 3 on the receiver side. Note that 0 represents BPSK modulation scheme, 01 indicates that the modulation scheme is changed from BPSK to QPSK. Considering the combination of encoder and modulator according to the HMM states, for simplicity, BPSK and QPSK are used here, the modulation scheme is changed relying on the CNR estimated by CSI. The threshold of switching modulation scheme pattern is shown in Table 3. In this case, we desire a BER of less than 10^{-4}. The value 10^{-4} is chosen in order to determine the threshold of switching modulation scheme pattern. This threshold should be decided considering the demodulator selection error, i.e., when this demodulator selection error is constant for all the channel models, the threshold is also constant. Let the information data length be 50 bits, the code rate be $R = 0.5$. Therefore, using a convolutional (7, 5) code, the number of encoded bits is 100. The uncoded pilot symbols with bit length 10 are added to each packet, and transmitted using BPSK. The encoder and modulator switching sequence $\hat{x}(x_1, x_2, \cdots, x_{time})$ lengths are considered to be 25, 49, and 100. The number of iterations of the EM algorithm is from 1 to 6.

Table 3 Threshold for adaptive modulation scheme.

BPSK - QPSK
Es/No=7 (dB)

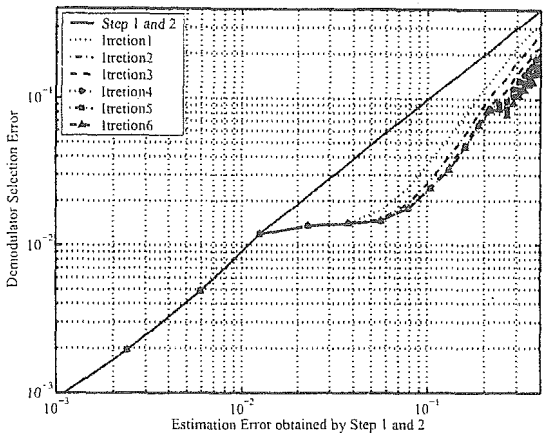

Fig. 5 Demodulator selection error in case switching sequence length is 25.

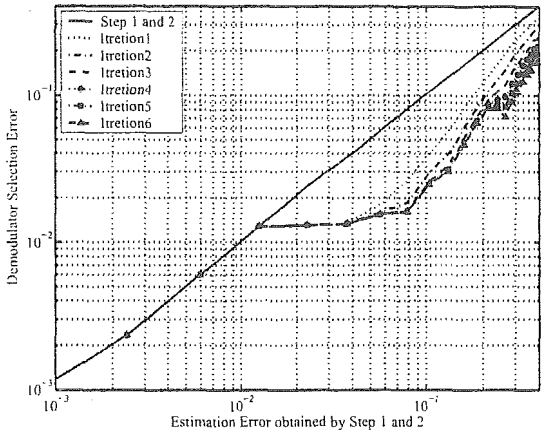

Fig. 6 *Demodulator selection error in case switching sequence length is* 49.

Figures 5–8 show computational evaluation for demodulator selection error considering CM1 channel model compared with estimation error at Step 1 and 2 in Fig. 3. In Figs. 5–7, it is seen that the system converges at less than the 6-th iteration with the EM algorithm. The complexity of proposed system considers $6n$ sequences, while the maximum likelihood estimation system selecting all the combinations of any sequence considers 2^n sequences to estimate the most probable sequence. Therefore, the proposed system is effective when $n \geq 5$. Additionally, as far as time permits, the longer the sequence length is, the lower the decoder and demodulator selection errors are. Moreover, we can see an error floor at around 10^{-2}, this means that there is a limitation to reduce the modulation selection error by using proposal method.

Compared with estimation error at Step 1 and 2 in

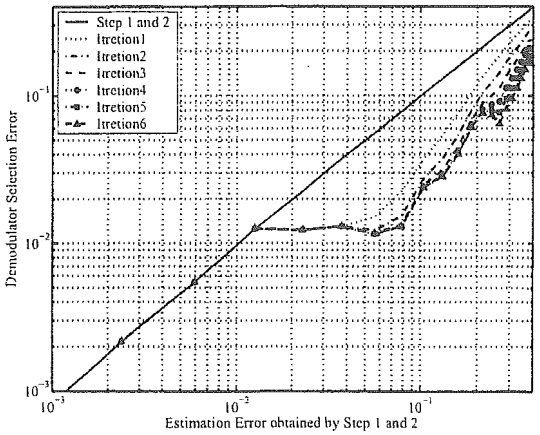

Fig. 7 Demodulator selection error in case switching sequence length is 100.

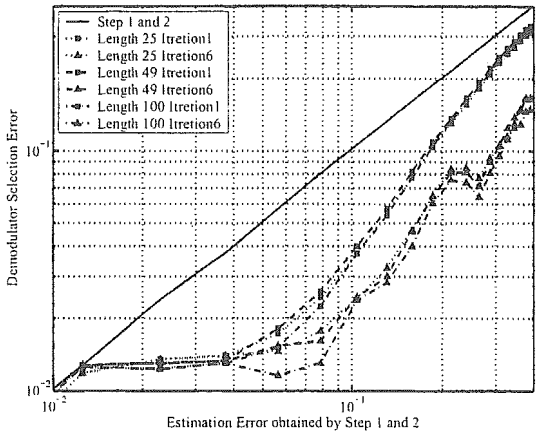

Fig. 8 Demodulator selection error compared with switching sequence length.

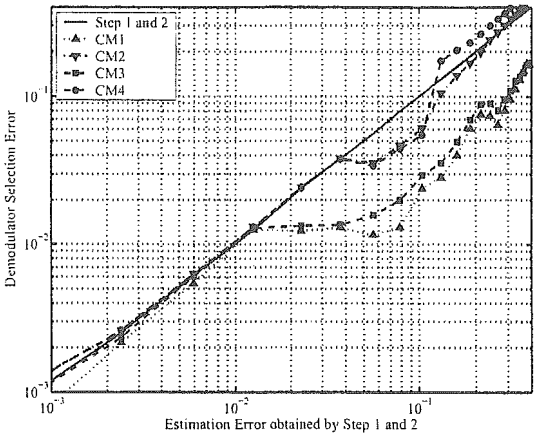

Fig. 9 Demodulator selection error considering channel models of CM1-CM4.

Fig. 3, Fig. 9 shows demodulator selection error considering CM1-CM4 channel models. Note that the number of iterations of the EM algorithm is 6. It is seen that the performance using CM1-CM4 achieves lower demodulation selection error compared with estimation error at Step 1 and 2. Moreover, we can see that the performance of CM1 and CM3 channel model achieves lower demodulation selection error than that of using CM2 and CM4. It means that system considering both CM2 and CM4 channel model selects BPSK and QPSK randomly and this characteristic is hard to distinguish bad state 0 from good state 1 of the HMM in (8). In terms of the threshold of switching modulation pattern described above, due to the difference of demodulator selection error according to the channel models in Fig. 9, we decide this threshold to achieve a BER less than 10^{-4} in order to show our proposed scheme is effective even though it is in the worst case. We utilize this threshold to change the modulation scheme in transmitter and estimate the modulation scheme in receiver to obtain the demodulator estimation error such as Fig. 9. As a result, it is proved that our proposed scheme is effective in any channel model. The details are shown below. In proposed system, we assume that the modulation scheme changes between BPSK and QPSK considering CM1 and CM3 channel models in Fig. 9. In this case, we can see that the proposed system achieves the BER of less than $2 \cdot 10^{-2}$ when the estimation error is from 10^{-1} to $2 \cdot 10^{-2}$ obtained by Step 1 and 2. On the other hand, when we assume the same modulation switching pattern for CM2 and CM4 channel models is used as that for CM1 and CM3 in Fig. 9, it is seen that the proposed system also achieves the BER of less than 10^{-1} when the estimation error is from 10^{-1} to $4 \cdot 10^{-2}$ obtained by Step 1 and 2. Moreover, in the future work, we shall concentrate on reducing the error floor of our proposed system to meet lower BER.

4. Conclusion

In this paper, a reduction of decoder and demodulator selection errors scheme is proposed using HMM as an elemental technology to achieve adaptive channel coding and modulation schemes. Based on channel estimation results, the proposal estimates the sequences such as encoder or decoder switching pattern at the transmit side using the probabilities of decoder and demodulator selection errors that are obtained by the switching pattern and channel information. Especially, we proposed a maximum likelihood estimation scheme in order to estimate the most likely switching patterns by EM algorithm, and then evaluated the performances by computer simulations. Comparing to the scheme only considering channel estimation results, the proposed scheme achieves better performance, and the computational complexity to search the encoder and modulator switching pattern sequence is lowered from 2^n to $6n$, which is effective when $n \geq 5$. In the future, we will investigate the balance of pilot symbols and information bits, and also the number of encoder or modulator switching pattern sequences that are needed to estimate HMM at the receiver.

References

[1] H. Matsuoka, S. Sampei, and N. Morinaga, "Adaptive modulation system with punctured convolutional code for high quality personal communication systems," IEICE Trans. Commun., vol.E79-B, no.3, pp.328–334, March 1996.
[2] T. Ue, S. Sampei, N. Morinaga, and K. Hamaguchi, "Symbol rate and modulation level-controlled adaptive modulation/TDMA/TDD system for high-bit-rate wireless data transmission," IEEE Trans. Veh. Technol., vol.47, no.4, pp.1134–1147, Nov. 1998.
[3] A. Swami and B.M. Sadleer, "Hierarchial digital modulation classification using cumulants," IEEE Trans. Commun., vol.48, no.3, pp.416–429, March 2000.
[4] H. Yoshioka, Y. Shirato, M. Nakasugawa, and S. Kubota, "Automatic modulation recognition techniques employing the nearest neighbor rule," IEICE Trans. Commun. (Japanese Edition), vol.J84-B, no.7, pp.1176–1162, July 2001.
[5] K. Umebayashi and R. Kohno, "Blind estimation of modulation schemes according to noise powers in the presence of carrier frequency offset," IEICE Trans. Commun. (Japanese Edition), vol.J84-B, no.7, pp.1151–1161, July 2001.
[6] K. Umebayashi, R.H. Morelos-Zaragoza, and R. Kohno, "Method of non-data-aided carrier recovery with modulation identification," IEICE Trans. Fundamentals, vol.E87-A, no.3, pp.656–665, March 2004.
[7] K. Ikemoto and R. Kohno, "Adaptive channel coding scheme using finite state machine for software defined radio," IEICE Trans. Commun., vol.E85-B, no.12, pp.2663–2671, Dec. 2002.
[8] W. Turin and R. van Nobelen, "Hidden Markov modeling of flat fading channels," IEEE J. Sel. Areas Commun., vol.16, no.9, pp.1809–1817, Dec. 1998.
[9] C. Anton-Haro, J.A.R. Fonollosa, C. Fauli, and J.R. Fonollosa, "On the inculusion of channel's time dependence in a hidden Markov model for blind channel estimation," IEEE Trans. Veh. Technol., vol.50, no.3, pp.867–873, May 2001.
[10] G.J. McLachlan and T. Krishnan, The EM Algorithm and Extensions, A Wiley-Interscience Publication, John Wiley & Sons, 1996.
[11] C.N. Georghiades and J.C. Han, "Sequence estimation in the presence of random parameters via the EM algorithm," IEEE Trans. Commun., vol.45, no.3, pp.300–308, March 1997.
[12] T.K. Moon, "The expectation-maximization algorithm," IEEE Signal Process. Mag., pp.47–60, Dec. 1996.
[13] C.N. Georghiades and D.L. Snyder, "The expectation-maximization algorithm for symbol unsynchronized sequence detection," IEEE Trans. Commun., vol.39, no.1, pp.54–61, Jan. 1991.

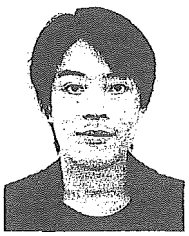

Kentaro Ikemoto was born in Saitama, Japan, in 1976. He received the B.E. and M.E. degrees in Electrical and computer engineering from Yokohama National University, Yokohama, Japan, in 2000 and 2002, respectively. He is currently studying toward Ph.D. degree in Electrical and computer engineering from Yokohama National University, Yokohama. His research interests include adaptive coding and modulation for digital mobile communication systems. He is a member of the IEEE.

Ryuji Kohno received the Ph.D. degree from the University of Tokyo in 1984. Dr. Kohno is currently a Professor of the Division of Physics, Electrical and Computer Engineering, Yokohama National University. In his currier he was a director of Advanced Telecommunications Laboratory of SONY CSL during 1998–2002 and currently a director of UWB Technology institute of National Institute of Information and Communications Technology (NICT). In his academic activities, he was elected as a member of the Board of Governors of IEEE Information Theory (IT) Society in 2000 and 2003. He has played a role of an editor of the IEEE Transactions on IT, Communications, and Intelligent Transport Systems (ITS). He is a vice-president of Engineering Sciences Society of IEICE and has been the Chairman of the IEICE Technical Committee on Spread Spectrum Technology, that on ITS, and that on Software Defined Radio(SDR). Prof. Kohno has contributed for organizing many international conferences, such as an chair-in honor of 2002 & 2003 International Conference of SDR(SDR'02 & SDR'03), a TPC co-chair of 2003 International Workshop on UWB Systems(IWUWBS'03), and a general co-chair of 2003 IEEE International Symposium on IT (ISIT'03), that of Joint UWBST&IWUWB'04 and so on. He was awarded IEICE Greatest Contribution Award and NTT DoCoMo Mobile Science Award in 1999 and 2002, respectively.

PAPER Special Section on Ultra Wideband Systems

Design and Analysis of Synthesized Template Waveform for Receiving UWB Signals

Kentaro TANIGUCHI[†a)], *Student Member and* Ryuji KOHNO[†b)], *Fellow*

SUMMARY Ultra Wideband (UWB) communication system utilizing impulse signals is attractive technique which can achieve high data rate with low complexity and low power consumption. In this impulse based UWB system, lots of different shaped pulses have been considered to represent more information bits per symbol. In order to detect these different shaped UWB signals at the receiver, the synthesized template generation method using several elementary waveforms is effective. In this paper we design and analyze this synthesized template waveform instead of the conventional matched filter technique. The synthesis of UWB template waveform can be achieved as combinations of orthogonalized elementary waveforms with Fourier coefficients. By adjusting the number of elementary waveforms and their coefficients, it is possible to detect several types of UWB signals. The orders of approximation corresponding to different number of elementary waveforms are analyzed and the bit error rate properties are then investigated in AWGN and multipath fading channels. In addition, the proposed system can capture more energy by adjusting its coefficients adaptively under the multipath environment and reduce the effect of Intra-Pulse Interference (IPI) which is occurred when the propagation channel is not separable, that is, multipath components spaced closer than the typical pulse width. We show the design of the adaptive template synthesis method and its performance compared with conventional Rake receiver.

key words: UWB, ultra wideband, template waveform, synthesis, elementary waveform, adaptive template

1. Introduction

Ultra-Wideband (UWB) has recently been investigated for wireless communications, as a candidate for multimedia wireless personal area networking (WPAN). UWB wireless system can provide high data rate and high capacity, it is therefore attractive for future communications. There exist two dominant technologies for UWB. One is the multiband technique that uses modulated signals to fall into the desired bandwidth, and the other, which is the one considered here, is the classic Impulse Radio (UWB-IR) technique that uses sub-nanosecond pulses [1], [2].

There are many pulse waveforms that have been investigated for UWB-IR, such as the Gaussian monocycle [1], the Modified Hermite Pulse (MHP) [3], [4]. While the Gaussian monocycle is generally used for Pulse Position Modulation (PPM) with random sequences, modified Hermite pulses are designed for implementing an M-ary Pulse Shape Modulation (PSM) scheme [3], [4]. Other orthogonal polynomials have also been researched to produce such orthogonal pulse shapes [6], [7].

To detect these UWB pulses, conventional receiver generally adopts matched filter technique, namely it is required to generate the template pulse that has the same pulse shape as the received one. Therefore it can detect only the designated UWB pulse, but not another type of UWB signal. In addition, the PSM scheme using orthogonal pulses such as the modified Hermite pulse has one disadvantage that it demands distinct sets of waveform generators at transmission and reception. On the other hand, there are some schemes about adaptive UWB pulse generation. A Soft-Spectrum-Adaptation (SSA) UWB transferring scheme is based on adaptive pulse waveform shaping with the merits of co-existence, interference avoidance [8], [9]. The multi-carrier based template waveform has been studied for interference reduction [10], [11]. These types of adaptive pulse shaping techniques can be considered the synthesis of UWB pulse waveform using some orthogonal elementary waveforms. By using a number of elementary waveforms, it becomes possible to detect several types of UWB signals derived from different kernel functions. From this point of view, we have analyzed the synthesis of template waveform in UWB-IR communications [12]. By adjusting the weight of each subcarrier, the sub-optimal template waveform can be synthesized which can detect different shaped UWB pulses. In this paper, we investigate the synthesized template waveform which is based on the approximation using some orthogonalized elementary waveforms weighted by coefficients vector.

Each UWB signal can be decomposed into Fourier coefficients, and it is therefore possible for the proposed receiver to detect different shaped impulse by adjusting the number of elementary waveforms and their coefficients appropriately.

And even in the multipath environment, the synthesized template can approximate the received UWB signal which is distorted through the channel. The performance of Rake receiver, which has been studied for multipath channel, degrades when the propagation channel is not separable, that is, multipath components spaced closer than the typical pulse width. Under such circumstances, the proposed template synthesizer can be performed by adjusting its coefficients vector to capture more energy from the received pulse adaptively. We show the enhancement of the proposed template synthesis method under IEEE UWB multipath channel

Manuscript received August 16, 2004.
Manuscript revised December 8, 2004.
Final manuscript received March 28, 2005.

[†]The authors are with the Division of Electrical and Computer Engineering, Faculty of Engineering, Yokohama National University, Yokohama-shi, 240-8501 Japan.
a) E-mail: kentarou@kohnolab.dnj.ynu.ac.jp
b) E-mail: kohno@ynu.ac.jp

DOI: 10.1093/ietfec/e88–a.9.2299

model called CM1 [13].

This paper is organized as follows. In Sect. 2, we describe the system model considered in this paper. The proposed template synthesis method and its theoretical analysis are discussed in Sect. 3. In Sect. 4, the degree of approximation and the required number of elementary waveforms for template synthesis are analyzed. Finally in Sect. 5, we draw some conclusions.

2. UWB Detection System

In this paper, we analyze the template synthesis method using several orthogonal elementary waveforms. The degree of synthesis has been investigated, and the bit error rate (BER) performances have been shown both in AWGN channel and in multipath channel.

2.1 AWGN Channel

In this section we describe the typical UWB-IR detection system. In the classic UWB system using impulse sequences, the transmitted UWB waveform is given as

$$s(t) = \sqrt{P} \sum_{i=-\infty}^{\infty} b_i a(t - iT_r) \tag{1}$$

where $a(t)$ is the equivalent RF pulse shape, b_i are the modulated data symbols, T_r is the pulse repetition period, and P is the transmitted power of the impulse. The modulated symbols are assumed to be bipolar (i.e., $b_i \in \pm 1$), and the transmitted waveform is normalized as follows

$$B_s \int_{-\infty}^{\infty} a^2(t)dt = 1 = B_s \int_{-\infty}^{\infty} |A(f)|^2 df \tag{2}$$

where B_s is the occupied bandwidth of the waveform and $A(f)$ is the Fourier transform of $a(t)$.

In AWGN channel, the received waveform can be written as follows:

$$r(t - t_0 - \tau) = \alpha s(t - t_0 - \tau) + n(t) \tag{3}$$

where $n(t)$ is the AWGN with two-sided power spectral density $N_0/2$, τ is the time delay between transmitter and receiver clocks, t_0 is the transmitted time and α is the path loss. As shown in Eq. (3), the description for user is omitted for simplicity. The path loss factor α ia normalized as $\alpha = 1$ and any distortive effects that antennas and channel introduce in UWB communication are removed from consideration. On the receiver side, as shown in Fig. 1(a), the received signal $r(t)$ is generally correlated with the expected template waveform $w(t)$ that matches to the transmitted pulse waveform.

$$D_i = \int_{-\infty}^{\infty} r(t)w(t)dt \tag{4}$$

If the correlated output D_i is greater than zero, then a positive symbol is decided as the transmitted one. If the correlated output is less than zero, then a negative symbol is decided instead of the positive one. In the case of PSM scheme

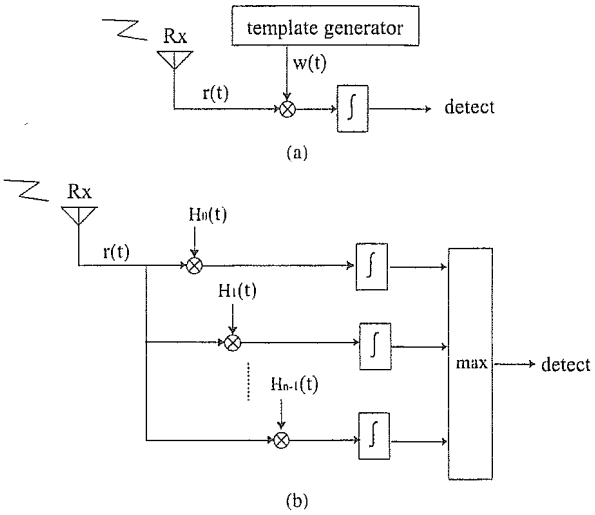

Fig. 1 Conventional receiver structures (a) in Pulse-Position-Modulated-UWB (PPM-UWB) system (b) in PSM-UWB system.

using modified Hermite pulse, each transmitted symbol is one of the N orthogonal Hermite pulses which is given by [4]

$$H_n(t) = (-1)^n e^{\frac{t^2}{2}} \frac{d^n}{dt^n} e^{-t^2} \tag{5}$$

where n is the order of Hermite polynomial. The orthogonality of Hermite pulses can be described as

$$\int_{-\infty}^{\infty} H_n(t)H_m(t)dt = \begin{cases} 0 & \text{if } (n \neq m) \\ 2^n n! \sqrt{\pi} & \text{if } (n = m) \end{cases} \tag{6}$$

We assume that perfect synchronization between transmitter and receiver exists. This means that codewords can be detected in a symbol-by-symbol maximum likelihood fashion using a correlation between the received signal and each of the N orthogonal pulses. The correlation output $\phi_n(t)$ corresponding to the n-th codeword is given by

$$\phi_n(t) = \int_{-T/2}^{T/2} r(t)H_n(t)dt \tag{7}$$

where T is duration time of Hermite pulse [5]. Receiver structure of PSM scheme is illustrated in Fig. 1(b).

As shown in Fig. 1, the general UWB receiver is required to generate a template waveform that matches to the transmitted waveform, and is unable to detect another type of UWB signal. In addition, the need for distinct sets of waveform generators at reception in PSM system leads to complexity. As shown in Sect. 3, we consider a synthesized template waveform produced with a set of locally generated waveforms, without matched filter technique.

2.2 Multipath Channel

In addition to the consideration of AWGN channel, we also analyze the effects of realistic UWB indoor multipath fading channel, namely IEEE 802.15.3 modified S-V(Saleh-Valenzuela) channel model. The modified S-V channel

model has been recently proposed by the IEEE 802.15.3 Study Group (SG3a) and summarized from extensive indoor UWB channel measurements [13]. The proposed IEEE 802.15 S-V multipath model has been given as the following, in discrete time impulse response:

$$h(t) = X \sum_{l=0}^{L} \sum_{k=0}^{K} \alpha_{k,l} \delta(t - T_l - \tau_{k,l}) \tag{8}$$

where X is the multipath gain magnitude which is lognormally distributed, $\alpha_{k,l}$ are the multipath gain coefficients, T_l is the delay of the lth cluster, $\tau_{k,l}$ is the delay of the kth muptipath component relative to the lth cluster arrival time T_l. The channel coefficients are defined as follows: $\alpha_{k,l} = p_{k,l}\beta_{k,l}$, where $p_{k,l}$ is equally likely to take on the values of ± 1, $\beta_{k,l}$ is the lognormal fading term. The inter-cluster times between various clusters and rays are exponentially distributed. The channel coefficients are normalized as $h(t) = X \sum_{l=0}^{L} \sum_{k=0}^{K} \alpha_{k,l}^2 = 1$ in order to remove the path loss factor from consideration. There are four different models, namely from CM1 to CM4, for different distances of transmission and LOS (Line of Sight) or NLOS (Non-LOS). The received UWB signals transferred through the above-mentioned S-V multipath channel (Eq. (8)) can be described as

$$r(t) = X \sum_{l=0}^{L} \sum_{k=0}^{K} \alpha_{k,l} s(t - T_l - \tau_{k,l}) + n(t) \tag{9}$$

where $n(t)$ is the AWGN as mentioned above.

Here we apply another parameter m to represent the number of each multipath component, that is, we replace $\alpha_{k,l}$ with α_m, and $T_l + \tau_{k,l}$ with $m\tau_p$, where τ_p denotes a minimum path resolution time. Then the received UWB signal is rewritten as

$$r(t) = X \sum_{m=0}^{M} \alpha_m s(t - m\tau_p) + n(t) \tag{10}$$

where $M = (K + 1)(L + 1)$ represents the total number of resolvable multipath components for each signal.

At the receiver side, we consider Partial-Rake (P-Rake) diversity combining using the information on the first L_p paths, and Selective-Rake (S-Rake) diversity combining using the maximum L_p paths. The conventional Rake receiver uses a bank of correlators followed by a Rake combiner as shown in Fig. 2. There exist multiple Rake fingers which independently track different reflections of the channel to capture the energy in the multipath components. The received UWB signal $r(t)$ is correlated at each correlator with different time-shifted template waveforms. Overall, the whole time of correlations performed by several Rake fingers covers the signal delay period caused by various multipath components. Under the assumption that the perfect synchronization between transmitter and receiver, the correlation output of each Rake finger corresponding mth path of the ith symbol is described as

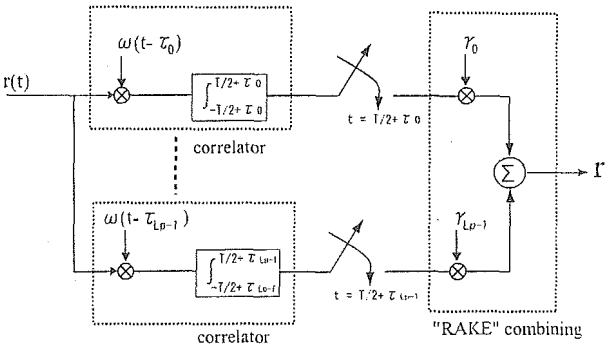

Fig. 2 Conventional Rake receiver architecture.

$$y_i^m = \int_{-\frac{T}{2}+(iT_r+m\tau_p)}^{\frac{T}{2}+(iT_r+m\tau_p)} r(t)w(t - iT_r - m\tau_p)dt \tag{11}$$

where $w(t)$ is expected template waveform (i.e., $w(t) = a(t)$) and $iT_r + m\tau_p$ are the relative delays. This correlation output can be rewritten as $y_i^m = d_i^m + n_i^m$, where each term corresponds to the desired signal and additive noise, respectively. If the propagation channel is separable (i.e., $T < \tau_p$), and the Inter Symbol Interference (ISI) effects are not considered, the desired term d_i^m is described as follows.

$$\begin{aligned} d_i^m &= \sqrt{P}Xb_i\alpha_m \int_{-\frac{T}{2}}^{\frac{T}{2}} a(t)w(t)dt \\ &= \frac{\sqrt{P}Xb_i\alpha_m}{B_s} \end{aligned} \tag{12}$$

The above equation is based on the assumption that there is no Intra-Pulse Interference (IPI), i.e.,

$$\int_{-\frac{T}{2}}^{\frac{T}{2}} w(t - i\tau_p)w(t - j\tau_p)dt = 0 \quad \text{for all } i \neq j \tag{13}$$

In this paper, however, we consider the effects of IPI, namely the received pulses are overlapping (i.e., $T > \tau_p$). In this case, the pulse shape is distorted through the channel. We denote Q the number of multipath components within pulse width, that is, $Q = \lfloor \frac{T}{\tau_p} \rfloor$ (here, the notation $\lfloor x \rfloor$ denotes the integer part of x). Then the desired term of the correlation output of each Rake finger corresponding mth path of the ith symbol is described as

$$\begin{aligned} d_i^m &= \sqrt{P}Xb_i \sum_{j=0}^{Q} \left\{ \alpha_{m+j} \int_{-\frac{T}{2}}^{\frac{T}{2}} a(t)w(t - j\tau_p)dt \right\} \\ &= \sqrt{P}Xb_i \sum_{j=0}^{Q} \{\alpha_{m+j} R_{aw}(j\tau_p)\} \end{aligned} \tag{14}$$

where

$$R_{aw}(\tau) = \int_{-\frac{T}{2}}^{\frac{T}{2}} a(t)w(t - \tau)dt \tag{15}$$

In Eq. (14), the terms for $i = 1, \cdots, Q$ represent the effects

of IPI. In this case, the transmitted waveform $a(t)$ is not appropriate to be used as the template waveform $w(t)$ at the receiver because of the distortive effects caused by IPI.

The noise term in the output of the Rake finger corresponding mth path of the ith symbol is described as follows.

$$n_i^m = \int_{-\frac{T}{2}}^{\frac{T}{2}} a(t)n(t)dt \tag{16}$$

Here, n_i^m are independent, Gaussian distributed random variables with a zero mean and variance $\sigma^2 = N_0/2B_s$ for all m and i.

The output of ith symbol at the Rake receiver can be described as

$$r_i = \sum_{m=0}^{L_p-1} \gamma_m \cdot y_i^m \tag{17}$$

where L_p is the number of Rake finger and γ_m is the weight of mth Rake finger determined by channel estimation. The bit decision is made as following:

$$b_i = \begin{cases} 1 & \text{if} \quad (r_i \geq 0) \\ 0 & \text{if} \quad (r_i < 0) \end{cases} \tag{18}$$

In this paper, channel estimation can be achieved using training sequence b_k $(k = 0, 1, \cdots, P-1)$ comprising P pilot symbols. The estimated path gain of the mth path can be written as follows:

$$\hat{h}_m = \frac{1}{P} \sum_{k=0}^{P-1} b_k \hat{y}_k^m \tag{19}$$

where $\hat{y}_k^m$ is the correlation output corresponding mth path of the kth pilot symbol. Applying the Maximum Rate Combining (MRC) at the Rake receiver, the weight of each Rake finger corresponding mth path is equal to the estimated path gain.

$$\gamma_m = \hat{h}_m \tag{20}$$

3. Proposed Scheme Description

3.1 Design of Synthesized Template Waveform

In this paper we analyze the template synthesis method for UWB receiver, in which template waveform is constructed as combinations of orthogonalized elementary waveforms with certain coefficients. The proposed receiver structure is illustrated in Fig. 3. It has some local elementary pulse generators and makes it possible to detect several types of UWB pulses by adjusting each coefficient properly. In this section, we describe this template synthesizer and show some analyses.

Generally, every UWB signal can be decomposed into some orthogonal elementary waveforms such as sine waves by Fourier series expansion independent of its kernel function. It is therefore possible to approximately construct

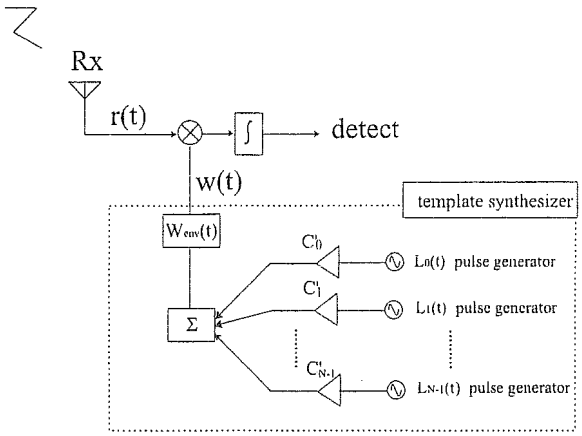

Fig. 3 Proposed receiver structure.

a UWB template waveform by expanding the UWB signal into the weighted sum of several orthogonal elementary waveforms and truncating it to finite order. If we consider an orthonormal set $\{L_k, k = 1, 2, \cdots, \infty\}$ in a Hilbert space S, L_k is complete under the condition that the following equation holds for every $w \in S$ [15].

$$w = \sum_{k=1}^{\infty} \langle w, L_k \rangle L_k \tag{21}$$

where the notation $\langle w, L_k \rangle$ denotes the inner product. Using this L_k as a set of basis functions, the waveform $w(t)$ is represented as

$$w(t) \approx \sum_{k=1}^{N} C_k L_k(t) \tag{22}$$

The set of coefficients $\{C_k, k = 1, 2, \cdots, N\}$ provides the best representation (in the least-squares sense) of $w(t)$. The minimum squared error of the series representation is

$$\left\| w - \sum_{k=1}^{N} C_k L_k \right\|^2 = \|w\|^2 - \sum_{k=1}^{N} \langle w, L_k \rangle^2 \tag{23}$$

Since the error is never negative, it follows that

$$\sum_{k=1}^{N} |C_k|^2 = \sum_{k=1}^{N} \langle w, L_k \rangle^2 \leq \|w\|^2 \tag{24}$$

This inequality is known as Bessel's inequality. If we use a complete set $\{L_k, k = 1, 2, \cdots, \infty\}$, there is no error in the representation, therefore Bessel's inequality becomes an equality,

$$\|w\|^2 = \sum_{k=1}^{\infty} |C_k|^2 \tag{25}$$

This relationship known as Parseval's equality shows that the waveform synthesized by complete set can strictly match to the ideal waveform. In this paper, the synthesized template waveform is described as

Substituting Eq. (32) to Eq. (31), the SNR after the correlator at the receiver is

$$SNR_{out} = \frac{P\left(1 - (MSE)^2 + \frac{(MSE)^4}{4}\right)}{N_0} \tag{33}$$

Since the cross-correlation between $r_s(t)$ and $w(t)$ is less than 1, the proposed template synthesizer performs worse in comparison with the matched filter based receiver. The bit error rate property, however, improves as the order of approximation, i.e. the number of elementary waveforms is increased. It is therefore fair to say that the performance of the matched filter based receiver is the lower bound on the synthesized template generation methods. According to Eq. (33), the bit error rate is given by

$$BER = \frac{1}{2} erfc \sqrt{\frac{P\left(1 - (MSE)^2 + \frac{(MSE)^4}{4}\right)}{2N_0}} \tag{34}$$

When $MSE = 0$, then $BER = 1/2 erfc \sqrt{P/2N_0}$, that is the theoretical BER characteristics of UWB-BiPhase in AWGN channel. The theoretical analyses of MSE and BER characteristics described above are only applicable to AWGN channel. Multipath channel requires other analysis, which is described in the following subsections.

3.3 Adaptive Template Synthesis Method in Multipath Channel

In multipath channel, the Rake receiver is supposed to be able to capture the signal energy spread over time. The long pulse width of the transmitted signal, however, has a great negative impact on the performance of Rake receiver. If there exists IPI, that is, the multipath components are distributed very closely in time within the typical pulse width, the Rake receiver doesn't perform well, for the channel distorts the signal waveform severely. The effect of IPI against the received signal is described in Eq. (14). On the assumption that the multipath componets of the received signal is distributed with the same time interval τ_p and the pulse width T is longer than τ_p, the waveform of the received singal is far from the transmitted one even if there is no effects of AWGN or ISI. This distortive effect is greatly increased as the pulse width is getting longer compared with τ_p. Figure 5 shows the degradation of correlation output d_i^m in Eq. (14) at the Rake receiver when the pulse width is changed. As in Eq. (14), the correlation is performed between the transmitted pulse $a(t)$ and the received pulse $r(t)$ through multipath channel (IEEE 802.15.3 UWB indoor multipath channel model, CM1 [13]). The correlation value is normalized to have a unit energy when $T = \tau_p$ for simplicity. The correlation window is the same time duration T as the pulse width, and the minimum path resolution time τ_p is 0.167 [ns]. The change of pulse width from $T = 0.167$ [ns] to 3.0 [ns] in Fig. 5 is equivalent to $1 \le Q \le 18$ in Eq. (14). It can be seen from Fig. 5 that the correlation output decreases

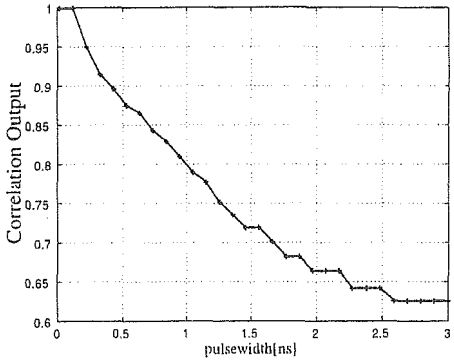

Fig. 5 Pulse width vs. correlation output at the 1-finger S-Rake receiver (without ISI and Noise). Minimum path resolution time $\tau_p = 0.167$ [ns].

as the pulse width becomes large compared with path resolution time τ_p. In such circumstances, we propose an adaptive template synthesis method which can generate suboptimal template waveform to capture more energy from the received pulse adaptively.

As mentioned above, in multipath environment the receiver needs to estimate the path gain. We consider the training sequence b_k $(k = 0, 1, \cdots, P + \acute{P} - 1)$ comprising $P + \acute{P}$ pilot symbols in each packet, where the first P symbols are used for the path gain estimation and the last $\acute{P}$ symbols are used for the synthesis of template waveform. The correlation output at the certain finger of Rake receiver corresponding to the mth multipath component of the kth pilot symbol is

$$\hat{y}_k^m = \int_{-\frac{T}{2}+(kT_r+m\tau_p)}^{\frac{T}{2}+(kT_r+m\tau_p)} r(t)w(t - kT_r - m\tau_p)dt \tag{35}$$

In order to estimate the path gain $\hat{h}_m$ corresponding the mth multipath component, the arithmetic average of the correlation outputs $\hat{y}_k^m (k = 0, \cdots P-1)$ is figured out as described in Eq. (19). From this estimation, the maximum multipath gain $\hat{h}_M = \max\{\hat{h}_m | m \in [0, M]\}$ and its relative delay τ_M within each time frame are derived. Therefore the most preferable time to capture the signal energy within each time frame T_r is supposed to be $\tau_M \le t \le \tau_M + T$. In the proposed scheme, the receiver extracts this time duration out of the received signal corresponding to the $\acute{P}$ pilot symbols to synthesize template waveform. The extracted signals of each pilot symbol can be written as $\{r_k(t) | kT_r + \tau_M \le t \le kT_r + \tau_M + T, k \in [P, P + \acute{P} - 1]\}$. We describe this highly amplitude received signal as the $(n \times 1)$ vector form.

$$\mathbf{r}_k = [r_{k1}\ r_{k2}\ \cdots\ r_{kn}]^t \quad (\text{for } k = P, \cdots, P + \acute{P} - 1) \tag{36}$$

where n is the number of samples during $\tau_M \le t \le \tau_M + T$ within each time frame. In order to synthesize the optimal template waveform that can capture more enegy from the set of distorted received signals $\mathbf{r}_k$, we derive the appropriate coefficients vector $\acute{\mathbf{C}} = [\acute{C}_1\ \acute{C}_2\ \cdots\ \acute{C}_N]$ for which the function

Table 1 Elementary waveforms and their orthogonality (δ_{mn} is the Kronecker delta).

Kind of functions	Elementary waveforms $L_n(t)$	Orthogonality
Trigonometric ($f_n = \frac{n}{T}$)	$\exp(j2\pi f_n t)$	$\int_{-\frac{T}{2}}^{\frac{T}{2}} L_n(t)L_m(t)dt = T\delta_{mn}$
Modified Hermite	$(-1)^n e^{\frac{t^2}{2}} \frac{d^n}{dt^n} e^{-t^2}$	$\int_{-\infty}^{\infty} L_n(t)L_m(t)dt = 2^n n! \sqrt{\pi}\delta_{mn}$
Modified Laguerre	$\frac{e^{\frac{t}{2}}}{n!} \frac{d^n}{dt^n}(t^n e^{-t})$	$\int_{0}^{\infty} L_n(t)L_m(t)dt = \delta_{mn}$
Legendre	$\frac{1}{2^n n!} \frac{d^n}{dt^n}(x^2-1)^n$	$\int_{-\infty}^{\infty} L_n(t)L_m(t)dt = \delta_{mn}$

$$w(t) = \sum_{k=1}^{N} \acute{C}_k \int_{-\frac{T}{2}}^{\frac{T}{2}} L_k(t) \times W_{env}(t)dt \tag{26}$$

where $L_k(t)$ are the orthogonal elementary waveform and $\acute{C}_k$ are the corresponding coefficients. $W_{env}(t)$ is the envelope which truncates each elementary waveform to finite duration. Rectangular window is used as $W_{env}(t)$, that is

$$W_{env}(t) = rect(\tau) = \begin{cases} 1 & (|t| \leq \frac{T}{2}) \\ 0 & (\text{others}) \end{cases} \tag{27}$$

Generally, the coefficients C_k are derived as follows

$$C_k = \frac{2}{T} \int_{-\frac{T}{2}}^{\frac{T}{2}} r_s(t)L_k(t)dt \tag{28}$$

where T is the pulse duration. As mentioned above, if the set of orthogonal elementary waveform $L_k(t)$ is complete, the synthesized template strictly matches to the ideal one. In reality, however, the number of coefficients and elementary waveforms should be finite. The coefficient vector $\mathbf{C}$ whose element is described as Eq. (28) is truncated to finite order by using the function $\hat{F}(N, \mathbf{C})$. The function $\hat{F}(N, \mathbf{C})$ selects the subset which consists of N-tuple chosen from vector $\mathbf{C}$ in descending order of magnitude. Therefore, the coefficient vector used to synthesize the template waveform is written as $\acute{\mathbf{C}} = \hat{F}(N, \mathbf{C}) = [\acute{C}_1\ \acute{C}_2\ \cdots\ \acute{C}_N]$. We consider four orthogonal functions as elementary waveform $L(t)$, that is, trigonometric function, modified Hermite polynomial, modified Laguerre polynomial and Legendre polynomial. The mathematical description of each function and its orthogonality is shown in Table 1.

Figure 4 shows the spectrum of proposed template waveform constructed by 3 elementary waveforms, which synthesizes modulated Gaussian UWB pulse described as following

$$r_s(t) = \cos(2\pi f_k t) \times \exp\left(-a \cdot \left(\frac{t}{\tau_m}\right)^2\right) \tag{29}$$

where $f_k = 6.85$ [GHz], $a = \log_e 10$, $\tau_m = 0.45$ in Fig. 4. It can be seen from Fig. 4 that proposed template waveform can well approximate the ideal modulated UWB signal. In Fig. 4, we apply trigonometric function as elementary waveform for synthesis.

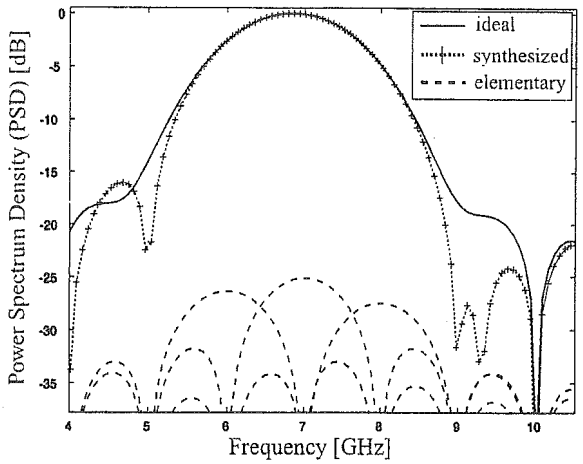

Fig. 4 Spectrum of synthesized template waveform constructed by 3 elementary waveforms. Ideal UWB signal is modulated Gaussian pulse with center frequency 6.85 [GHz].

3.2 MSE and BER Characteristics

In this subsection, the theoretical analysis of proposed template in AWGN channel is described. The synthesized template waveform does not match strictly to the ideal UWB signal, therefore there exists the reconstruction error. As one of the evaluation measure for the waveform synthesis, we apply normalized Mean Square Error (MSE) described as follows:

$$MSE = \sqrt{\frac{\int_{-\frac{T}{2}}^{\frac{T}{2}} (r_s(t) - w(t))^2 dt}{\int_{-\frac{T}{2}}^{\frac{T}{2}} r_s(t)^2 dt}} \tag{30}$$

where $r_s(t)$ is desired signal term of the received signal, $w(t)$ is synthesized template. In Eq. (30), the effects of AWGN and multipath are removed from consideration. MSE is the ratio between the squared sum of the reconstruction error and the squared sum of the ideal waveform. If there is no error, MSE equals zero. The degree of approximation of our proposed template depends on the number of orthonormal basis used for synthesis, namely MSE decreases as the number of orthonormal basis increases. The received signal $r(t)$ is correlated with the synthesized template waveform $w(t)$. The Signal to Noise Ratio (SNR) after correlation can be expressed as

$$SNR_{out} = \frac{PR_{r_s w}^2(\tau)}{N_0 R_{ww}(0)} \tag{31}$$

where $R_{r_s w}(\tau)$ and $R_{ww}(0)$ is defined by Eq. (15). We assume perfect synchronization between transmitter and receiver and $r_s(t)$ and $w(t)$ are normalized to have a unit energy, therefore $\tau = 0$, $R_{ww}(0) = 1$. From Eq. (30), $R_{r_s w}(\tau)$ is described as follows in AWGN channel.

$$R_{r_s w}(\tau) = \frac{2 - (MSE)^2}{2} \tag{32}$$

$$F = \sum_{k=P}^{P+\acute{P}-1} |\langle \mathbf{r_k}, \mathbf{w} \rangle|^2 \tag{37}$$

is maximum, where $\mathbf{w}$ is vector based description of template waveform $w(t)$, whose size is $(n \times 1)$ [14]. We set $\mathbf{w}$ to be of unit energy for normalization purposes and it is rewritten in vector representation as follows.

$$\mathbf{w} = \sum_{j=1}^{N} \acute{C}_j \mathbf{L}_j \tag{38}$$

The above equation is equivalent to Eq. (26). $\mathbf{L}_j$ denotes the orthonormal basis used to synthesize the template waveform and it is also written in vector form as follows:

$$\mathbf{L}_j = [L_{j1}\ L_{j2}\ \cdots\ L_{jn}]^t \quad (\text{for } j = 1, 2, \cdots N) \tag{39}$$

where N is the number of orthonormal basis used for synthesis and each orthonormal basis consists of n samples. For instance, if we use trigonometric function as basis, then $\mathbf{L}_k = \exp(j2\pi f_k u)$, $u \in [1, n]$. Here, we set an $(n \times N)$ matrix $\mathbf{M}$ whose jth column is $\mathbf{L_j}$, that is

$$\mathbf{M} = [\mathbf{L_1}\ \mathbf{L}_2\ \cdots\ \mathbf{L_N}] \tag{40}$$

In this case, $\mathbf{w}$ in Eq. (38) reduces to

$$\mathbf{w} = \mathbf{M} \cdot \acute{\mathbf{C}}^t \tag{41}$$

We also set an $(n \times \acute{P})$ matrix $\mathbf{A}$ whose kth column is $\mathbf{r_k}$, that is

$$\mathbf{A} = [\mathbf{r_1}\ \mathbf{r}_2\ \cdots\ \mathbf{r_{\acute{P}}}] \tag{42}$$

From Eq. (41) and Eq. (42), it can be derived that $\mathbf{w}^t \cdot \mathbf{A}$ forms $(1 \times \acute{P})$ vector, whose kth element is $\langle \mathbf{r_k}, \mathbf{w} \rangle$. Therefore

$$\begin{aligned} F &= \sum_{k=P}^{P+\acute{P}-1} |\langle \mathbf{r_k}, \mathbf{w} \rangle|^2 \\ &= (\mathbf{w}^t \cdot \mathbf{A}) \cdot (\mathbf{w}^t \cdot \mathbf{A})^t \\ &= (\acute{\mathbf{C}} \cdot \mathbf{M}^t \cdot \mathbf{A}) \cdot (\mathbf{A}^t \cdot \mathbf{M} \cdot \acute{\mathbf{C}}^t) \end{aligned} \tag{43}$$

Eq. (43) can be transformed as

$$F = \acute{\mathbf{C}} \cdot (\lambda \cdot \acute{\mathbf{C}}^t) = \lambda \cdot \|\acute{\mathbf{C}}\|^2 \tag{44}$$

where λ is eigen value of $(N \times N)$ square matrix $(\mathbf{M^t} \cdot \mathbf{A}) \cdot (\mathbf{A^t} \cdot \mathbf{M})$. In order to make the function F maximum, the eigen value in Eq. (44) should be maximum. Therefore the optimal coefficients vector $\acute{\mathbf{C}}$ is supposed to be simply the normalized eigen vector of matrix $(\mathbf{M^t} \cdot \mathbf{A}) \cdot (\mathbf{A^t} \cdot \mathbf{M})$ corresponding to its largest eigen value. By using $\acute{P}$ pilot symbols included in each packet, the coefficients vector $\acute{\mathbf{C}}$ is derived adaptively as shown in Eq. (43) and Eq. (44). The template waveform can be synthesized using this coefficient vector $\acute{\mathbf{C}}$ as described in Eq. (41).

4. Simulation Results

In this section we present some simulation results and analysis about the template synthesis method for UWB communications.

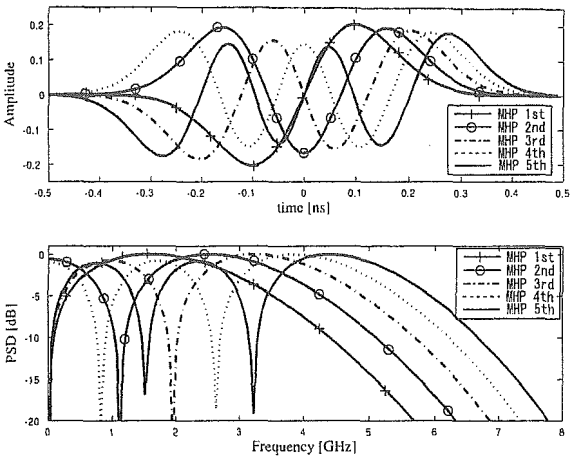

Fig. 6 Modified Hermite Pulse (MHP) waveform in time and frequency domain.

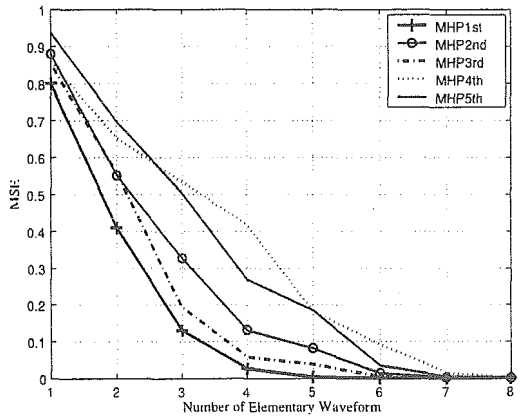

Fig. 7 MSE characteristics of synthesized MHP waveforms (from 1st to 5th as described in Fig. 6) when the number of trigonometric elementary waveform is increased. (pulse width T = 1.0 [ns])

4.1 MSE and BER Characteristics in AWGN Channel

In this paper, MHP of order 1st to 5th are considered as the transmitted UWB signal. Any distortive effects that antennas introduce in UWB communication are removed from consideration. The MHP waveforms both in time and frequency domain are shown in Fig. 6. MHP is the smooth function both in time and frequency domain and easily derived from transformation of the Gaussian pulse. It can be seen from Fig. 6 that the pulse width and bandwidth of each MHP is different. These waveforms are just derived from Eq. (5). First, we show the MSE characteristics of these normal MHP synthesized by several elementary waveforms based on trigonometric function in Fig. 7. The Fourier fundamental period is 1 [ns]. Note that any noise effect is not considered in MSE characteristics. MSE just means the degree of approximation between the ideal waveform and synthesized waveform. It can be seen from Fig. 7 that the MSE decreases as the number of elementary waveforms is

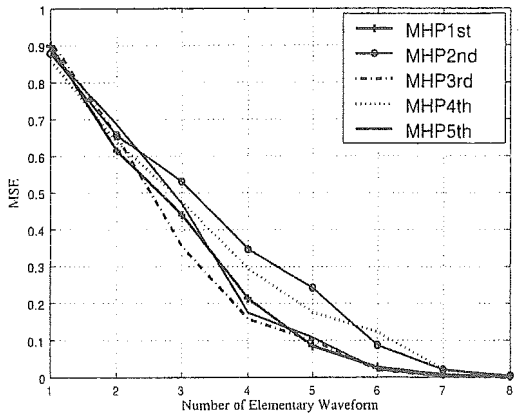

Fig. 8 MSE characteristics of synthesized MHP waveforms. Each MHP has the same bandwidth 3.2 [GHz]. (pulse width $T = 2.0$ [ns])

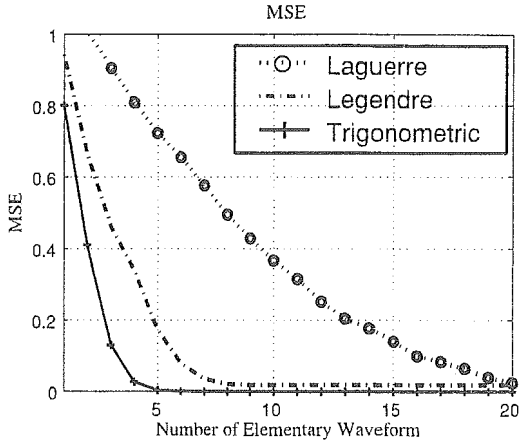

Fig. 9 The difference of MSE characteristics based on three kinds of elementary waveforms, trigonometric function, Modified Laguerre polynomial and Legendre polynomial. The 1st order MHP is synthesized. (pulse width $T = 1.0$ [ns])

increased. The required number of elementary waveform to achieve $MSE = 0$ for all MHP is $N = 7$. Due to the fact that the MSE characteristics are highly depends on the bandwidth of synthesized pulse in applying trigonometric function to synthesis, the curves for different order MHP perform differently. In order to adjust the frequency bandwidth of MHP, we adopt new parameter α and rewrite Eq. (5) as follows:

$$H_n(t) = (-1)^n e^{\frac{t^2}{2\alpha^2}} \frac{d^n}{dt^n} e^{-(\frac{t}{\alpha})^2} \tag{45}$$

By adjusting α for each MHP, it is possible to make each MHP have the same bandwidth. The MSE characteristics of these adjusted MHP are shown in Fig. 8. The -10 [dB] bandwidth of All MHP are 3.2 [GHz] and the parameter α of each MHP are $2.1, 2.45, 2.7, 2.9, 3.1$ respectively. The difference of each MSE curve is smaller than that of Fig. 7. The waveform synthesized by trigonometric function is a type of multicarrier based waveform. Therefore its MSE characteristics mainly depend on the bandwidth of each signal.

The difference of MSE characteristics based on three kinds of elementary waveforms, trigonometric function, Modified Laguerre polynomial and Legendre polynomial is shown in Fig. 9. The 1st order MHP whose pulse width is $T = 1.0$ [ns] is synthesized. It can be seen that the MSE characteristics highly depend on the elementary waveform used for synthesis. Every MSE curve shows exponential decay, which indicates that these elementary waveforms can be used as complete sets to synthesize template waveform. The required number of elementary waveforms to achieve small MSE depends on the correlation value between ideal waveform and each elementary waveform. If we consider $a(t) = \sum_{i=0}^{\infty} C_i L_i(t)$ as ideal waveform, the distribution of correlation value between $a(t)$ and each orthogonal basis $L_i(t)$ ($i \in [0, \infty]$), is derived as the following inductive functions.

$$\hat{C}_i = \max_n \left\{ \int_{-\frac{T}{2}}^{\frac{T}{2}} A_i(t) L_n(t) dt \right\} \text{ for } \forall n \in [0, \infty] \tag{46}$$

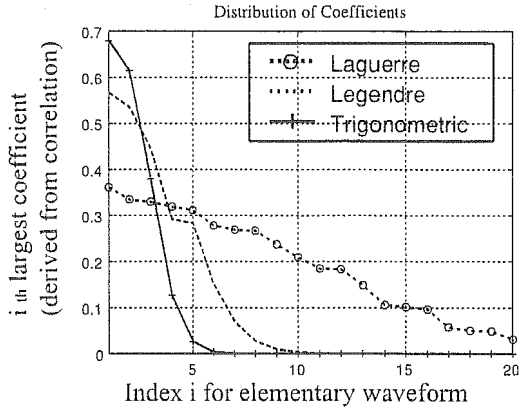

Fig. 10 Distribution of coefficients vector $\hat{C}$. Three different orthogonal basis are considered to synthesize the 1st order MHP.

$$I_i = \underset{n}{\text{argmax}} \left\{ \int_{-\frac{T}{2}}^{\frac{T}{2}} A_i(t) L_n(t) dt \right\} \text{ for } \forall n \in [0, \infty] \tag{47}$$

$$A_i(t) = A_{i-1}(t) - \hat{C}_{i-1} L_{I_{i-1}}(t) \tag{48}$$

$$\hat{C}_0 = 0,\ I_0 = 0,\ A_0(t) = a(t)$$

where $\hat{C}_i$ denotes the ith largest coefficient value corresponding to a certain elementary waveform whose order is I_i. Figure 10 shows the distribution of coefficient vector $\hat{C}_i$ ($i \in [1, 20]$), where these three orthogonal basis are considered to synthesize the 1st order MHP. It can be seen from Fig. 10 that the trigonometric function has a few large valued coefficients compared with other basis, which reduces the required number of elementary waveform for synthesis as shown in Fig. 9. Due to tha fact that the waveform of Modified Laguerre polynomial has great fructuation unlike trigonometric function and Legendre polynomial, the required number for synthesis is quite large.

According to Fig. 7, the MSE value corresponding the template waveform synthesized by certain number of ele-

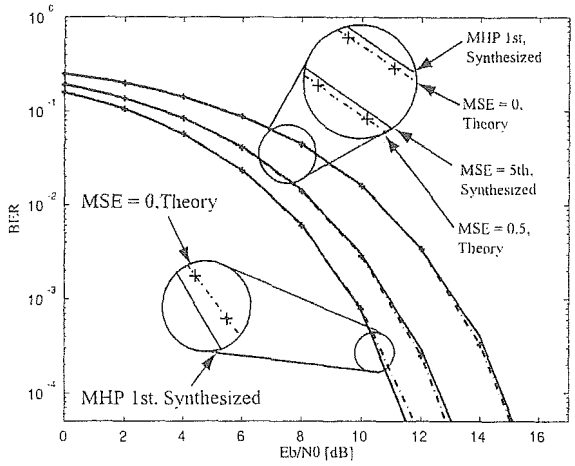

Fig. 11 The comparison of BER performance between simulation results and theoretical curves for UWB-BiPhase in AWGN channel.

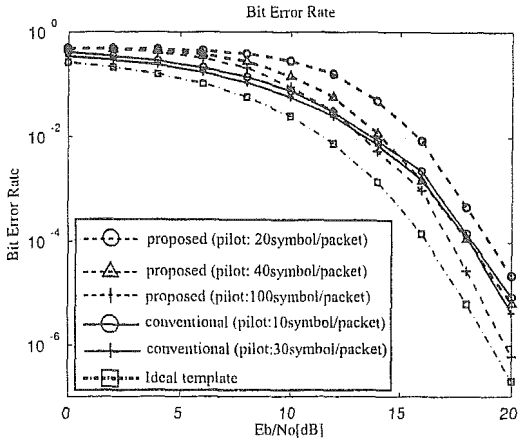

Fig. 12 BER characteristics of the proposed template waveform with different pilot symbols. As for proposed system, 20 symbols per packet means 10 symbols for estimation and 10 symbols for synthesis. 40 symbols per packet means 10 symbols for estimation and 30 symbols for synthesis. 100 symbols per packet means 10 symbols for estimation and 90 symbols for synthesis.

mentary waveforms can be found. The theoretical BER performance of certain MSE value is derived from Eq. (34). The comparison of BER performance between simulation results and theoretical curves for UWB-BiPhase in AWGN channel are shown in Fig. 11. Theoretical curve of MSE = 0 is compared with simulation result where 1st order MHP synthesized by 6 elementary waveforms based of trigonometric function is applied as template waveform at the receiver. MHP pulse width is $T = 1.0$ [ns] and one pulse represents one symbol. Note that ideal synchronization is assumed between the transmitter and receiver during the simulation procedures. Analogously, theoretical curve of MSE = 0.5 and 0.8 are compared with 5th order MHP template synthesized by 3 elemenatary waveforms and 1st order MHP template synthesized by 1 elementary waveform respectively. The number of elementary waveform for synthesis are derived from Fig. 7. It can be seen from Fig. 11 that each theoretical curve of certain MSE value has the same performance with the simulation results using synthesized template waveform at the receiver.

4.2 Adaptive Template Synthesis Method

In multipath channel, we mainly consider Intra-pulse Interference (IPI) problem which is occurred when the multipath components are distributed more closely than typical pulse width. We analyze the adaptive template method mentioned above, and show some simulation results. As multipath model, we apply IEEE 802.15.3 UWB indoor multipath channel model (CM1), and assume that the channel delay profile remains time-constant during the transferring process of each packet. As a packet constitution, we consider several pilot symbols and 1000 data symbols for each packet. Each pulse represents one symbol and pulse repetition period is assumed to be long enough to ignore ISI. The transmitted UWB pulse $a(t)$ is always assumed to be the 2nd order MHP whose pulse width is $T = 1.67$ [ns] and template waveform is synthesized adaptively for each packet by using trigonometric function. 100 channel realization are used and 1 packet including pilot and data symbols are transmitted for each channel realization at each value of noise. At the proposed receiver, only results from the single major Rake finger are always considered (i.e., S-Rake with 1-finger). In Fig. 12, the "ideal template" curve means that the receiver knows the channel information perfectly and uses template waveform which is strictly matches to the received waveform distorted by IPI, and correlated at the right moment with the proper coefficient. Figure 12 shows the BER characteristics of the proposed template waveform with different pilot symbols for each packet. Both of the conventional and proposed receiver are assumed to be S-Rake receiver with 1 finger. The proposed system uses 20, 40 and 100 pilot symbols per each packet in which the first 10 symbols are used for estimation of maximum path gain and the other symbols are used for synthesis. It can be seen from Fig. 12 that the performance of conventional system little depends on the number of pilot symbols because these pilot symbols are used for the estimation of only one maximum path gain. On the other hand, the proposed system depends on the number of pilot symbols greatly due to the fact that the adaptive synthesis of template waveform is achieved by reference of several pilot symbols and the effect of AWGN is mitigated as the number of reference symbol is increased. It is impossible for the conventional receiver to show the same performance with the ideal template as shown in Fig. 12 because of the existence of mismatch between the template waveform and the received signal distorted by the effects of IPI. The proposed system can achieve the performance of the ideal template by using several pilot symbols to synthesize the desired waveform under the high SNR region. In low SNR region, due to the fact that the proposed system refers severely distorted pilot signal for synthesis, the performance gets worse. Therefore some compensation techniques are

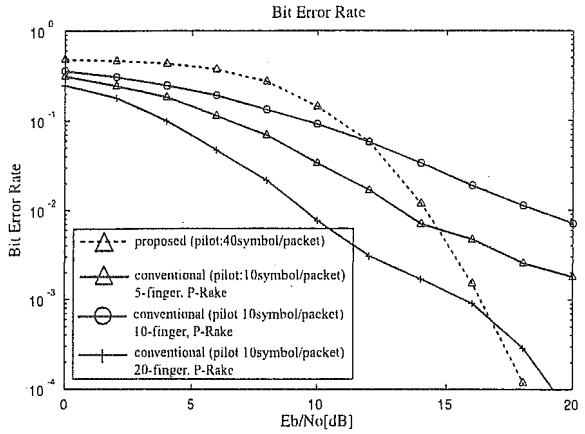

Fig. 13 The comparison of BER characteristics between the proposed template method and the conventional P-Rake receiver with 5, 10, 20 finger. (Both system use 10 pilot symbols per packet for path gain estimation. In addition, proposed system uses more 30 pilot symbols for template synthesis.)

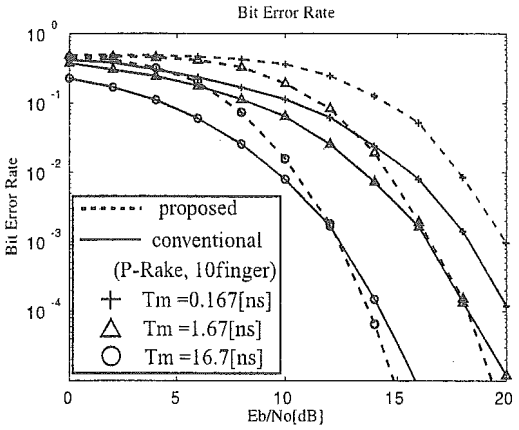

Fig. 14 BER characteristics of the proposed system and the conventional P-Rake receiver when the pulse width is changed to T = 0.167, 1.67, 16.7 [ns].

required in low SNR region, like equalization or synchronized summation. The switching method from conventional template to adaptively synthesized template depending on SNR is also effective.

Figure 13 shows the difference of BER performance when the number of finger at the conventional P-Rake receiver is changed. It is assumed that the both system use 10 pilot symbol per packet for path gain estimation. In addition, proposed system uses more 30 pilot symbols for template synthesis. As the number of finger increases at the conventional system, the performance gets better, and the SNR area where the proposed system can show the effectiveness gets smaller. While the proposed system highly depends on the number of pilot symbols as shown in Fig.12, it can be seen from Fig. 13 that the performance of conventional receiver highly depends on the number of Rake finger. On the other hand, Fig. 14 shows the difference of BER characteristics when the transmitted pulse width is changed. Both of the proposed and conventional system uses 20 pilot symbols for each packet and the number of P-Rake finger of conventional detector is 10. The proposed receiver uses more 20 pilot symbols per packet to synthesize the template. As the pulse width is getting wider, the correlation window becomes wide, which lead to better performance for both system. The degree of improvement of performance in high SNR region is remarkable for the proposed adaptive template system. The proposed method enables the received system to have more ability in the sense that it becomes possible to achieve the same performance as the precisely matched filter even in the multipath environment.

5. Conclusions

In this paper the template synthesis method for detecting several types of UWB received signals is analyzed. This system uses a set of locally generated elementary waveforms to synthesize UWB signals. We show the number of elementary waveforms to attain the desired performance. In constructing the synthesized template waveform, several orthogonal functions, such as trigonometric function, Laguerre polynomial and Legendre polynomial are considered. We have found that by using any orthogonal function, it is possible to detect several types of UWB signals and bit error rate performances come close to that of the matched filter based detector. This template generation technique for UWB communications allows to detect any UWB signal by adjusting the number of elementary waveforms and their coefficients appropriately without conventional matched filter technique. This property makes the proposed receiver so flexible.

In addition, we propose the adaptive template synthesis method in multipath channel. Under the condition that there is severe Intra-Pulse Interference, the proposed receiver can synthesize the suboptimal template waveform by using a number of pilot symbols.

In future we intend to investigate the performance of the proposed system when inter symbol interference is present.

References

[1] M.Z. Win and R.A. Scholtz, "Ultra-wide bandwidth time-hopping spread-spectrum impulse radio for wireless multiple-access communications," IEEE Trans. Commun., vol.48, no.4, pp.679–691, April 2000.
[2] M.Z. Win and R.A. Sholtz, "Impulse radio: How it works," IEEE Trans. Commun., vol.2, no.2, pp.36–38, Feb. 1998.
[3] M. Ghavami, L.B. Michael, and R. Kohno, "Hermite function based orthogonal pulses fro ultra wideband communications," Proc. WPMC'01, pp.437–440, Aalborg, Denmark, Sept. 2001.
[4] G.T.F. de Abreu, C.J. Mitchell, and R. Kohno, "On the orthogonality of Hermite pulses for ultra wideband communications systems," Proc. WPMC'03, pp.V2-288–292, Yokosuka, Japan, Oct. 2003.
[5] C. Mitchell, G.T.F. de Abreu, M. Hernandez, and R. Kohno, "Analysis of combined PPM and orthogonal pulse shape detection in UWB systems," Proc. WPMC'03, pp.V2-293–297, Yokosuka, Japan, Oct. 2003.

[6] M. Pinchas and B.Z. Bobrovsky, "Orthogonal laguerre polynomial pulses for ultra-wideband communications," Proc. IWUWBS'03, Oulu, Finland, June 2003.
[7] S. Ciolino, M. Ghavami, and H. Aghvami, "UWB pulse shape modulation system using wavelet packets," Proc. IWUWBS'03, Oulu, Finland, June 2003.
[8] http://grouper.ieee.org/groups/802/15/pub/2003/Jul03/03097r5P802-15TG3a-Communications-Research-Lab-CFPPresentation.ppt
[9] H. Zhang, T. Kobayashi, and R. Kohno, "On timing jitter and tracking of soft-spectrum UWB system in IEEE 802.15.3 multipath fading channel," Proc. WPMC'03, pp.V2-136–140, Kanagawa, Japan, Oct. 2003.
[10] K. Ohno and T. Ikegami, "Effect of interference from other radio system to UWB impulse radio," Proc. IWUWBS'03, Oulu, Finland, June 2003.
[11] K. Ohno, T. Ikebe, and T. Ikegami, "A proposal for an interference mitigation technique facilitating the coexistence of bi-phase UWB and other wideband systems," Proc. Joint UWBST&IWUWBS'04, pp.50–54, Kyoto, Japan, May 2004.
[12] K. Taniguchi and R. Kohno, "Design and analysis of template waveform for receiving UWB signals," Proc. Joint UWBST&IWUWBS '04, pp.125–129, Kyoto, Japan, May 2004.
[13] J. Foerster, "Channel modeling sub-comitee report final," IEEE P802.15 WG for WPANs Technical Report, no.02/490r0-SG3a, 2002.
[14] A. Taha and K.M. Chugg, "On designing the optimal template waveform for UWB impulse radio in the presence of multipath," Proc. UWBST'02, pp.41–45, Baltimore, U.S.A., May 2002.
[15] T.K. Moon and W.C. Stirling, Mathematical Methods and Algorithms for Signal Processing, Prentice Hall, 2000.

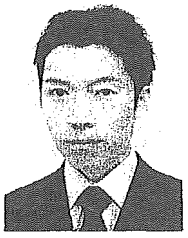

Kentaro Taniguchi received the M.S. degree in electrical and computer engineering from Yokohama National University, Yokohama, Japan, in 2005. He is currently working toward the Ph.D. degree in electrical and computer engineering at Yokohama National University, Yokohama, Japan. His research interests lie in the area of ultra wideband communication and information theory. He is a student member of IEEE.

Ryuji Kohno received the Ph.D. degree from the University of Tokyo in 1984. Dr. Kohno is currently a Professor of the Division of Physics, Electrical and Computer Engineering, Yokohama National University. In his career he was a director of Advanced Telecommunications Laboratory of SONY CSL during 1998–2002 and currently a director of UWB Technology institute of National Institute of Information and Communications Technology (NICT). In his academic activities, he was elected as a member of the Board of Governors of IEEE Information Theory (IT) Society in 2000 and 2003. He has played a role of an editor of the IEEE Transactions on IT, Communications, and Intelligent Transport Systems (ITS). He is a vice-president of Engineering Sciences Society of IEICE and has been the Chairman of the IEICE Technical Committee on Spread Spectrum Technology, that on ITS, and that on Software Defined Radio (SDR). Prof. Kohno has contributed for organizing many international conferences, such as a chair-in honor of 2002 & 2003 International Conference of SDR (SDR'02 & SDR'03), a TPC co-chair of 2003 International Workshop on UWB Systems (IWUWBS'03), and a general co-chair of 2003 IEEE International Symposium on IT (ISIT'03), that of Joint UWBST & IWUWBS'04 and so on. He was awarded IEICE Greatest Contribution Award and NTT DoCoMo Mobile Science Award in 1999 and 2002, respectively.

PAPER Special Section on Ultra Wideband Systems

Adaptive RAKE Receivers with Subspace-Based Hadamard-Hermite Template Design for UWB Communications

Craig J. MITCHELL[†a)], *Student Member*, Giuseppe ABREU[†*], *Member, and* Ryuji KOHNO[†], *Fellow*

SUMMARY In this paper we present a novel method for improving RAKE receiver reception in UWB systems. Due to the fact that practical pulses that can be produced for UWB-IR (Ultra Wideband-Impulse Radio) may occupy a longer time than the typical multipath resolution of the actual UWB channel, multiple channel components may arrive within this typical pulse width. Performance degradation may occur due to the resulting intrapulse (overlapping received pulses) interference. We here propose an adaptive, pilot aided RAKE receiver for UWB communications in the multipath environment. The proposed system estimates the actual received signal with intrapulse interference in each RAKE finger using projections onto a Hadamard-Hermite subspace. By exploiting the orthogonality of this subspace it is possible to decompose the received signal so as to better match the template waveform and reduce the effects of intrapulse interference. By using the projections onto this subspace, the dimension of the received signal is effectively increased allowing for adaptive correlator template outputs. RAKE receivers based on this proposal are designed which show significant performance improvement and require less fingers to achieve required performance than their conventional counterparts.

key words: *ultra wideband, RAKE receiver, multipath, orthogonal Hermite pulses*

1. Introduction

UWB systems have recently become a popular topic of research as they promise very high speed wireless communications with many advantages over conventional radio systems [1], [2]. Such systems offer the possibility of very low cost, high speed links over a short range (< 10 m). These links are hoped to support transmissions such as digital video while doing away with unsightly and inconvenient cables. Further possible applications include sensor networks and Personal Area Networks.

Typically UWB-IR systems communicate using trains of very short (1 ns or less) pulses with a very low duty cycle. The energy is thus spread over a wide range of frequencies or bandwidth, resulting in a low power density at any single frequency. The extremely wide bandwidth gives UWB systems their strength. One problem, however, is that the received signal suffers from a significant multipath environment with relative path delays that are shorter than the duration of a typical realistic pulse ([3]–[6]). This fact will lead to intrapulse interference, as received pulses will overlap due to the close arrival times of the multipath components. This in turn will adversely affect the performance of any correlation based receiver.

The high degree of path diversity that is present, on the other hand, can be utilized and exploited by using a RAKE like structured receiver (e.g. [7], [8]). Due to the fact that the inter-arrival times of the multipath components are not integer multiples of the pulse width, only a highly complicated fractionally spaced (FS) receiver utilizing maximum likelihood (ML) detection can compensate for the intrapulse interference that will be observed [8]. The problem with such receivers is that they are extremely complex and require sampling at least at the Nyquist rate (which is impractically high in UWB systems as it may be in the order of tens of Gigahertz). They also require perfect knowledge of all multipath component amplitude and arrival times and will therefore require complex channel estimation algorithms for any realistic implementation.

One alternative option recently considered to improve this situation is to use the Transmitted Reference (TR) system ([9], [10]). Here pulses are transmitted in pairs, an unmodulated reference pulse followed by the modulated data pulse. The resulting received reference waveform is stored and used as the correlation template for the following modulated data pulse. Such a system is seen to be quite energy inefficient as two pulses are needed per data symbol. In addition the reference received waveform needs to be stored in an analog manner for correlation with the modulated pulse. This may be impractical and inefficient in reality.

Simplified RAKE receivers are therefore still a definite candidate for UWB transmission, but will suffer not only from relatively high complexity (due to the number of fingers and correlators required) but also from inefficient energy capture due to intrapulse interference. In this paper we propose a fingerwise modification to the RAKE receiver which attempts to improve this intrapulse interference problem.

Orthogonal pulse designs, such as those based on Hermite functions have been proposed for use in UWB systems so as to implement M-ary Pulse shape modulation (PSM) [11]–[13]. Use of such orthogonal pulse shapes are, however, thought to be severely hampered by the multipath

Manuscript received August 3, 2004.
Manuscript revised November 26, 2004.
Final manuscript received February 25, 2005.

[†]The authors are with the Graduate School of Engineering, Division of Physics, Electrical and Computer Engineering, Yokohama National University, Yokohama-shi, 240-8501 Japan.
[*]Presently, with the Center for Wireless Communications, University of Oulu, Finland.
a) E-mail: Craig.Mitchell@kohnolab.dnj.ynu.ac.jp
DOI: 10.1093/ietfec/e88–a.9.2327

channel. Recently it is therefore thought that use of these orthogonal pulses is impractical for UWB. We here propose an alternative application of such orthogonal functions for intrapulse interference compensation in a RAKE Receiver. A set of such orthogonal pulses form an orthonormal basis which can be exploited in many circumstances. Many signals can be approximately reconstructed by decomposition onto such an orthogonal basis. We therefore propose to decompose the received signal in a given multipath environment in each finger of the RAKE using a *Hadamard-Hermite subspace*. The decomposed signals therefore represent reconstructions of the actual received signal, while at the same time increase the dimension of the received signal (to the size of the subspace) and allow the receiver to adapt its correlator template function closer to the actual received waveform. Instead of using the results of only one correlator for detection, use is now made of a bank of correlators, one for each of the orthogonal functions. This can be used to reduce the effect of intrapulse (intra-symbol) interference and increase the effective energy captured by the system.

The remainder of the paper is organized as follows. In Sect. 2 we introduce a brief background to the problem and discuss some relevant issues. In Sect. 3 we present our proposed system, in Sect. 4 we evaluate the performance of the system and present some simulation results and finally conclusions are given in Sect. 5.

2. The Multipath Channel and RAKE Receivers

2.1 Channel Model

A major concern in the implementation of any UWB system is the effect that the UWB multipath channel will have on performance. Much work has been carried out on channel measurements and modeling (e.g. [4]–[6]). A model that appears to have been widely accepted at this stage has been proposed by the IEEE P802.15.3a working group [3]. This model is based on the Saleh-Valenzuela model [14] with a couple of modifications. The model demonstrates a clustering phenomena of the multipath components into a number of discrete clusters. Each cluster in turn consists of a number of rays arriving in a certain spread of time. In addition it has been observed that each cluster exhibits independent fading as well as each ray within the cluster. This fading has also been seen to follow a log-normal distribution. The phase is randomly distributed to ± 1 representing channel inversions that may occur due to reflections of the waves off any solid objects. The model is represented by:

$$h(t) = X \sum_{l=0}^{L} \sum_{k=0}^{K} \alpha_{k,l} \delta(t - T_l - \tau_{k,l}), \quad (1)$$

where $\alpha_{k,l}$ are the gain coefficients, T_l is the arrival time of the lth cluster with $\tau_{k,l}$ being the relative arrival time of the kth ray within that cluster (relative to the first arrival path within the cluster ($\tau_{0,l}$). Both the cluster arrival rate and ray arrival rate are exponentially distributed, and the multipath gain magnitudes X are log-normally distributed. Four different models representing different distances of transmission with both LOS and NLOS ((Non)-Line of Site) have been proposed. Table 1 gives some of the most important channel parameters for these channel models labeled CM1-CM4.

Table 1 IEEE P802.15.3a working group channel model parameters, showing distance, line of sight, mean excess delay τ_m and RMS excess delay τ_{rms}.

Channel	CM1	CM2	CM3	CM4
Distance (m)	0–4	0–4	4–10	
(Non) Line of sight	LOS	NLOS	NLOS	NLOS
τ_m **(ns)**	5.05	10.38	14.18	
τ_{rms} **(ns)**	5.28	8.03	14.28	25

In this work the principles of design are introduced using models CM1 and CM2, representing both LOS and NLOS channels with a typical transmission distance of 0–4 meters. These channels together with CM3 represent the most likely application scenarios considered here, while CM4 is a long range outdoor channel. Simulation results will however show that similar improvements are also attainable in CM3 and CM4 using the proposed design.

We consider a multipath channel produced from the above model. One interesting thing to note about the UWB channel is that the multipath is quite dense, especially in the NLOS situation and may result in severe intrapulse interference. The pulse repetition time is considered to be much longer than the delay spread of the channel, thus avoiding intersymbol interference and giving a low probability of multiuser interference in the system.

2.2 RAKE Receivers

RAKE Receivers utilize the path diversity that is available in a multipath channel. This is achieved by splitting the received signal into a number of time components (fingers) for correlation. The conventional RAKE receiver consists of multiple correlators (termed fingers) which can extract the received signal at each different correlation time instant. Correlation is carried out using the expected received signal as the matched filter template. Conventionally each finger is positioned at the time instant of one of the resolved multipath components of the channel obtained by accurate channel estimation. The outputs of the fingers are then given appropriate weights and combined, using suitable combining methods, so as to obtain the advantages of multipath diversity [7], [8], [15]–[17].

Such a RAKE receiver can be implemented using a matched filter followed by a tapped delay line combiner with j taps. The number of taps in such an implementation is equal to the number of RAKE fingers and determines the instant in time that each correlation result is measured [15]. The RAKE system can resolve multipath components whose delays differ by at least one chip duration T_c (the RAKE resolution), which is typically the width of the template function or pulse width. The output of the correlator is therefore sampled at the time positions of the RAKE fingers

and combined appropriately.

The term all RAKE (ARake) refers to a receiver with unlimited resources [16], i.e. limitless fingers and path resolution. It attempts to position a finger at each and every resolved arrival path at the receiver so as to capture all of the impinging energy. This type of receiver also requires instant reconfiguration of the fingers for whenever the channel changes. Such a system is extremely complex, utilizes a large amount of power and is rather impractical. In reality each finger is of the order of a pulse width which is typically much larger than the multipath resolution. The performance of the correlators would suffer due to the intrapulse interference that results. One possible solution is to use many overlapping RAKE fingers, termed a Fractionally-Spaced RAKE (FSRake), together with the transmission of multiple pilot symbols so as to estimate the relative delays and magnitudes of all the paths accurately. This requires a large number of RAKE fingers and results in large complexity and energy issues in the combining procedure. Additionally overlapping fingers, as well as intrapulse interference will be limiting factors in such a receiver, as the chip duration is equal to the correlator template pulse duration ($T_c = T_p$). A typical RAKE combiner is therefore limited by power consumption, energy of the signals, design complexity and the channel estimation available.

Many reduced complexity RAKE designs exist, and in this paper we consider 2 broad types of reduced complexity RAKE receivers, namely the partial RAKE (PRake) and selective RAKE (SRake) [15]. The PRake assumes that the arrival time of the first path is known, the first finger is positioned at this instant and the rest of the fingers are then positioned at subsequent multiples of the finger resolution. The SRake first scans the multipath delay spread signal and selects the highest energy paths to position its fingers thereby capturing maximum energy for a given number of fingers.

In this paper we attempt to find an alternative solution to the typical RAKE receiver. We consider a system where perfect channel estimation is not available at the receiver. In addition we assume full independence between RAKE fingers, therefore no two fingers can overlap, implying a RAKE resolution that is equal to the pulse width. Effectively this is a situation when the RAKE resolution is lower than the multipath resolution. We also assume that the system uses maximum-ratio combining [18].

3. Proposed System

As mentioned before orthogonal pulse shapes and PSM have been proposed for use in UWB systems. Use of such orthogonal pulse shapes may be hampered by the multipath channel. The overlap of pulses due to the intrapulse interference will lead to severe loss of orthogonality and thereby, it is thought, render any PSM system useless. The feasibility of PSM seems to only be realizable when extremely short duration pulses (shorter than the multipath resolution—possibly some 10's of picoseconds) can be produced, thereby avoiding intrapulse interference and maintaining orthogonality. In this paper we will however show that such pulse shaping may still prove useful in detection for UWB systems.

3.1 RAKE Fingers

We propose a finger-wise modification of the RAKE receiver based on the decomposition of received signals using a Hadamard-Hermite orthonormal basis.

We assume that the transmitted pulse ω_{TR} is the traditional 1-st order Hermite pulse. Antenna effects are ignored or assumed to be compensated for (e.g. differentiating effects are compensated by the inclusion of integrators), so the received waveform $\omega_{RC} = \omega_{TR}$. It is noted that the transmit and receive antennas are known to differentiate the signal [12] (implying a second derivative received waveform), while the channel is believed to have an integration effect [19]. This means that we cannot produce any pulse lower than 0-th order and cannot receive one lower than 1-st order. This motivates the use of the 1-st order pulse here.

Using the 1-st order waveform means that the conventional RAKE receiver matched filter template function would be

$$T(t) = \omega_{RC}(t). \tag{2}$$

The proposal here is for a finger-wise improvement to the RAKE receiver system. Each finger in the RAKE receiver will follow the modifications that will here be proposed and described for a single major RAKE finger. This major finger is defined as one that is centered on the maximum magnitude received path for any given instance of the IEEE channel model.

The received signal in the absence of noise $p(t)$, for a finger of pulse width T centered at time t_0 is defined as

$$p(t) = \sum_{k=1}^{\upsilon} \alpha_k \omega_{RC}(t - t_m - \tau_k) \quad \tau \in \left[\frac{T_p}{2}; \frac{T_p}{2}\right], \tag{3}$$

where υ is the number of multipath components arriving in the duration of the finger (T_p) and α_k and τ_k represent the magnitude and relative delay of the k-th arrival path. t_m represents the mismatch between transmitter and receiver clocks. We assume perfect synchronization, so $t_m = 0$.

Figure 1(a) shows an example of the multipath channel components contained in such a major RAKE finger centered on the strongest multipath component and (b) shows the resulting received signal ($p(t)$) (composed of the weighted sum of shifted ω_{RC}) in the absence of noise for this finger. Also shown is the conventional RAKE finger template function $T(t)$ for comparison. As seen, multiple components may arrive within the pulse width (here assumed to be $T_p \approx 1$ ns) resulting in a mismatch between $p(t)$ and $T(t)$.

The RAKE finger performs detection by correlating the received waveform with the expected template.

$$\gamma(t) = \int_{-\frac{T}{2}}^{\frac{T}{2}} p(t)T(t - \tau)d\tau. \tag{4}$$

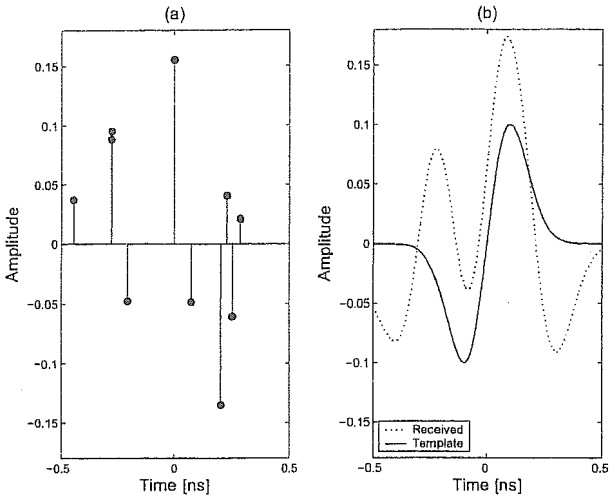

Fig. 1 (a) Example of major RAKE finger showing amplitudes and relative delays of the multipath components, (b) resulting noiseless received waveform ($p(t)$) and correlator template $T(t)$ in the major RAKE finger for channel shown in (a).

If we consider Antipodal Binary Pulse Amplitude Modulation (BPAM) (i.e. a "1" is represented by $\omega_{TR}(t)$ and a "0" by $-\omega_{TR}(t)$. Detection can be carried out as follows:

$$n_i = \begin{cases} 1 & \text{if} \quad \gamma(t) \geq 0 \\ 0 & \text{if} \quad \gamma(t) < 0 \end{cases} \tag{5}$$

The intrapulse interference can clearly be seen to have an effect on the performance of such a correlation procedure as the template $T(t)$ is not matched to $p(t)$, especially in the presence of noise. The closer the template $T(t)$ resembles the actual noiseless received signal $p(t)$ the better the performance would be, as optimal correlation is achieved when the signals match exactly.

3.2 Hadamard-Hermite Decomposition

The proposal in this paper is to use a Hadamard-Hermite subspace to decompose the received signal and more closely match the template to it.

Let the n-th order Hermite polynomial be defined in the interval $-\infty < t < \infty$ of a normalized time scale by the Rodrigues formula as follows [21]

$$P_n(t) \equiv (-1)^n e^{t^2} \frac{d^n}{dt^n} e^{-t^2} \quad n \in \mathbb{N}. \tag{6}$$

The normalized orthogonal Hermite pulses ψ_n are then defined by [12]:

$$\psi_n(t) = \frac{e^{\frac{-t^2}{2}} P_n(t)}{\sqrt{2^n n! \sqrt{\pi}}}, \tag{7}$$

where n is the order of the polynomial, and $n = 0, 1, \ldots$, $-\infty < t < \infty$. These pulses are orthogonal in time and have a number of attractive attributes. They are based on smooth functions which implies they can be feasibly produced, and are also well contained in both frequency and time. In addition closed form expressions for the cross correlation function for any pair (n, m) of such functions has also been found [12]:

$$\begin{aligned} R_{n,m}(\tau) &= \int_{-\infty}^{\infty} \psi_n(t)\psi_m(t-\tau)d\tau \\ &= \frac{(-1)^{2m+n}\tau^{m+n}\sqrt{n!m!}}{\sqrt{2^{m+n}}} e^{\frac{-\tau^2}{4}} \sum_{k=0}^{\lfloor (m,n) \rfloor} \frac{(-1)^k \tau^{-2k}\sqrt{4^k}}{(n-k)!(m-k)!k!} \end{aligned} \tag{8}$$

where $\lfloor (m, n) \rfloor$ denotes the minimum between n and m.

We further define the basis of Hadamard-Hermite pulses as follows. Consider an $n \times n$ Hadamard matrix $H = h_{i,j}$ where the entries $h_{i,j}$ are either $+1$ or -1 such that $HH^T = I^n$ where H^T is the transpose of H and I^n is the nth order identity matrix. Such a matrix H is defined as the nth order Hadamard matrix. The order of such a matrix is limited to 1, 2 or $4n$ where n is an integer. Given a Hadamard matrix H of order N, the normalized Hadamard-Hermite pulse is therefore defined as:

$$\varphi_n(t) = \frac{1}{\sqrt{N}} \sum_{k=0}^{N-1} h_{n,k}\psi_k(t), \tag{9}$$

Given the orthogonality of both H and $\psi_n(t)$ it follows that

$$\int_{-\infty}^{\infty} \varphi_m(t)\varphi_n(t)dt = \begin{cases} 0 & \text{if} \quad n \neq m \\ 1 & \text{if} \quad n = m \end{cases} \tag{10}$$

These Hadamard-Hermite pulses therefore form an orthonormal basis which we refer to as the *Hadamard-Hermite space*. The reason for using Hadamard-Hermites, as apposed to plain Hermites is to do with the effective utilization of energy and will become evident when the signal detection is considered in the next subsection. An improved template function ($T^*(t)$) which more closely approximates $p(t)$ can now be found if the projections of the received signal onto this Hadamard-Hermite space are used. Mathematically

$$p(t) \approx T^*(t) = \sum_{k=0}^{N-1} c_k\varphi_k(t). \tag{11}$$

The coefficients c_k are seen to be the cross correlation between the received signal $p(t)$ and the k-th order Hadamard-Hermite pulse $\varphi_k(t)$, i.e.

$$c_k = \int_{-\infty}^{\infty} \varphi_k(t)p(t)dt. \tag{12}$$

Solving this equation using Eq. (8) we find that the decomposed pulse more closely represents the received signal than the conventional $T(t)$. Figure 2(a) illustrates the reconstruction $T^*(t)$ of the received waveform $p(t)$, which was used

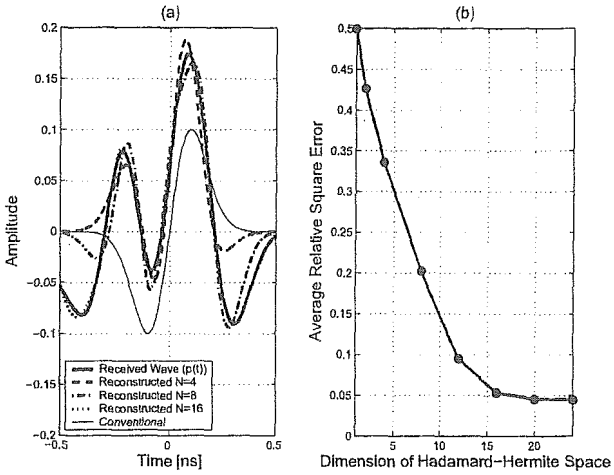

Fig. 2 (a) Reconstruction of $p(t)$ using Hadamard-Hermite space and (b) the average relative error in the reconstructed waveform in the major RAKE finger for different dimensions of Hadamard-Hermite space.

in Fig. 1, using different dimensions of Hadamard-Hermite space. As can be seen the waveforms obtained far closer resemble the actual $p(t)$ when compared to the conventional Template. For correlation purposes it can be seen that these waveforms are far more useful and would lead to improved performance when compared to the conventional template. Figure 2(b) shows a plot of the average relative square error in the reconstructed wave obtained from the major RAKE finger using 100 realizations of the IEEE CM1 channel model. Relative square error RSE, is calculated for sampled versions of p and T^* (with k samples) using,

$$RSE(T) = \frac{|p - T^*|}{|r|} = \sqrt{\frac{\sum_{j=0}^{k-1}(p(j) - T^*(j))^2}{\sum_{j=0}^{k-1} p(j)^2}}. \tag{13}$$

It is seen that the larger the dimension of the Hadamard-Hermite space the closer the reconstructed wave $T^*(t)$ resembles $p(t)$ and the lower the relative error is.

3.3 Signal Detection

The single matched filter of the RAKE Receiver is replaced with a bank of M correlators (each one consisting of a Hadamard-Hermite pulse from a dimension M Hadamard-Hermite space). We once again assume that BPAM modulation is being used. In the ideal noiseless case we see from Eq. (12) that the outputs of these correlators to an input $\omega_{RC}(t)$ would be,

$$\mathbf{c} = \{c_0, c_1, \ldots, c_{N-1}\}, \tag{14}$$

and if the input was $-\omega_{RC}(t)$ we would get $-\mathbf{c}$. In reality of course the system experiences noise and other distortions in both the channel and receiver hardware resulting in an actual received signal:

$$r(t) = p(t) + w(t) \tag{15}$$

where $w(t)$ is the additive noise and other interference. The outputs of the correlators with input $r(t)$ would now be:

$$\mathbf{d} = \{d_0, d_1, \ldots, d_{M-1}\}, \tag{16}$$

where

$$d_k = \int_{-\infty}^{\infty} \varphi_k(t) r(t) dt. \tag{17}$$

The proposed system uses the data-aided (DA) approach, where a number of known pilot symbols are transmitted at the beginning of the packet to estimate $\mathbf{c}$. The rest of the packet is decoded based on this estimated information. This is in accordance with the IEEE P802.15.3 UWB channel model which states that the channel is assumed to be time-invariant during the transmission of one packet if it is shorter that 200 μs. Channel realizations are also assumed to be independent between packets. Using $\mathbf{c}$ as the reference detection can now be carried out as follows:

$$n_i = \begin{cases} 1 & \text{if} \quad \mathbf{c} \cdot \mathbf{d}^T \geq 0 \\ 0 & \text{if} \quad \mathbf{c} \cdot \mathbf{d}^T < 0 \end{cases} \tag{18}$$

The dimension of the detection is effectively increased, as the outputs of all the M correlators are used in detection. This is advantageous to the performance of the system as was shown in [12].

3.4 Energy and Hadamard-Hermites

At this stage comment should be made about the use of a bank of Hadamard-Hermite as apposed to plain Hermite correlators. One undesirable consequence of using plain Hermite functions would be the sub utilization of the available energy. If we consider the "ideal" case where we have only one arriving pulse centered in the finger. If, in addition, ω_{RC} is the 1-st order Hermite pulse, then only one of the correlators in the bank of Hermites would output a value (i.e. c_1). All others would have zero outputs, which is sub-optimal, even though a single pulse centered within a finger should intuitively be the best situation. Under the same conditions, the Hadamard-Hermite bank would have non-zero output values on all its correlators.

An alternative explanation can be seen by looking at the decision process. Errors are effectively determined by the metric distance between the detection vector $\mathbf{c}$ and the vector of noise processes ω_n at each correlator output, i.e. the metric:

$$\Delta(\mathbf{c}, \sigma_\omega) = E\left[\left|\sum_{n=0}^{M-1} c_n\right| - \left|\sum_{n=0}^{M-1} \omega_n\right|\right], \tag{19}$$

where $E[\cdot]$ denotes expectation and it is assumed that all ω_n

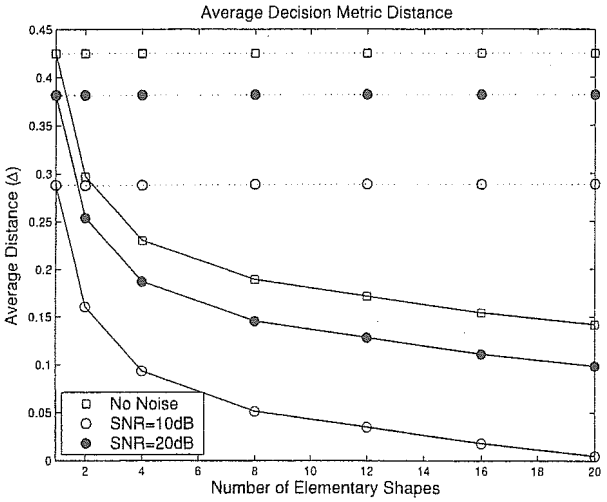

Fig. 3 Mean decision metric distance for plain Hermite (solid lines) and Hadamard-Hermites (dashed lines) with differing SNR values.

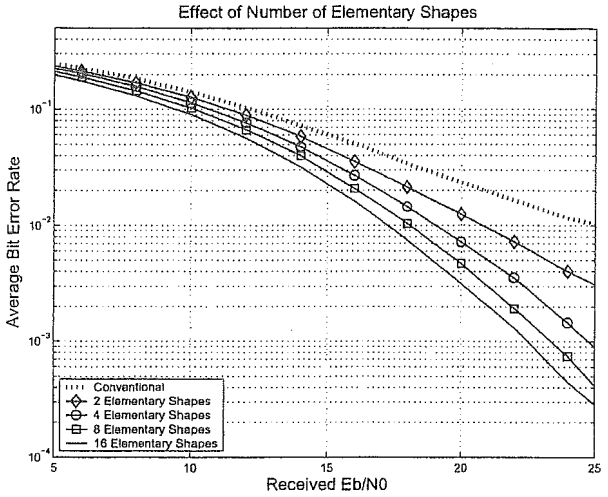

Fig. 4 Average bit error rate for major RAKE finger with increasing Hadamard-Hermite dimension.

are independent zero mean Gaussian processes with variance σ_ω. Figure 3 gives a plot of these metric distances comparing Hermites and Hadamard-Hermites at different SNR values obtained by measuring the average metric distance in the major RAKE finger considering 100 channel instances of CM1. It is clearly seen that the plain Hermites suffer from suboptimal utilization of the energy. The Hadamard-Hermite solution maintains the same mean distance regardless of the number of elementary shapes used. The advantages of the Hadamard-Hermite are therefore clear.

3.5 Subspace Size

We initially assume that perfect knowledge of the reference vector $\mathbf{c}$ is available. This can be obtained by transmitting suitable pilot symbols as will be seen in the next subsection. The payload length of each data packet is assumed to be 1024 bits.

One problem of course is the larger the size of the Hadamard-Hermite subspace, the more complex the resulting pulse shapes become (more zero crossings in a short space of time). These may prove difficult and impractical to accurately produce in reality. Using a very large subspace size may unnecessarily increase the complexity of the system implementation, possibly with little gain in performance. The effect of subspace size on the performance of the system needs to be investigated. To this end a system with a single major RAKE finger (as described before) is considered.

Figure 4 shows the Bit Error Rate performance of such a system with different sizes of Hadamard-Hermite space. The Received E_b/N_0 against which error rates are plotted is defined as the ratio between impinging energy (*per bit*) onto the receive antenna and the total noise at the output of the correlators. It can be seen that using a larger number of Hadamard-Hermite pulses improves the performance. One thing to note, however, is that the improvement in performance between 8 elementary shapes and 16 elementary shapes is relatively small. The increased complexity in using 16 as apposed to 8 shapes may make this impractical in a real system. The use of 8 shapes is therefore seen as a good compromise.

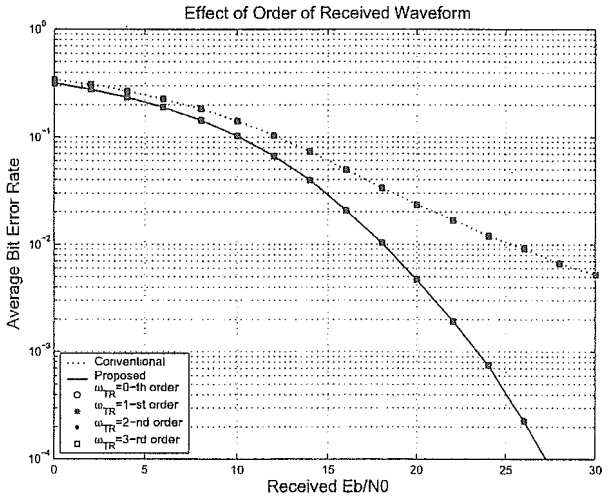

Fig. 5 Average bit error rate for major RAKE finger with increasing order of received waveform $\omega_{TR}(t)$ showing conventional (dashed line) and proposed system (solid line) using 8 elementary shapes.

As previously mentioned we are considering a received waveform $\omega_{RC}(t)$ that is the standard 1-st order Hermite pulse. It is noted that this can be substituted for any other order Hermite pulse. Figure 5 shows the effect in BER in the major RAKE finger using increasing orders of Hermite received waveform $\omega_{TR}(t)$. As can be seen all the waveforms give virtually identical BER performance (They cannot be distinguished). The system here presented is largely independent of transmit pulse order (Hermite pulses). A similar procedure can be followed for other different pulse shapes. Note these shapes may further be modulated so as to meet